INFLUENCE OF PARTICLE SIZE ON FLOW PROPERTIES OF BULK SOLIDS TESTED VIA A SCALED-UP JENIKE SHEAR CELL

By

SHREY GUPTA

A THESIS PRESENTED TO THE GRADUATE SCHOOL
OF THE UNIVERSITY OF FLORIDA IN PARTIAL FULFILLMENT
OF THE REQUIREMENTS FOR THE DEGREE OF
MASTER OF SCIENCE

UNIVERSITY OF FLORIDA

2009

To my family for their love, support and understanding

ACKNOWLEDGMENTS

I would like to thank Dr. Ray A. Bucklin for giving me the opportunity to conduct this study under his supervision. His enthusiasm, good-natured humor and patience motivated me in my efforts.

I would like to thank Dr. Kerry Johanson and Dr. Arthur A. Teixeira for their guidance, support and insightful remarks during the course of this study. I am especially indebted to Dr. Kerry Johanson whose course work helped me broaden my understanding and develop a passion for the subject.

I would also like to thank the staff of Agricultural and Biological Engineering especially, Steven R. Feagle and Billy W. Duckworth for their technical support.

I would like to express my deepest gratitude to my family. My father Vijay Gupta who has lovingly supported and encouraged me in all my endeavourers, my mother Soma Gupta for her love and affection and my brother Ankur Gupta who has been a tremendous influence on me and a great source of inspiration.

TABLE OF CONTENTS

LIST OF TABLES

LIST OF FIGURES

Abstract of Thesis Presented to the Graduate School
of the University of Florida in Partial Fulfillment of the
Requirements for the Degree of Master of Science

INFLUENCE OF PARTICLE SIZE ON FLOW PROPERTIES OF BULK SOLIDS TESTED VIA A SCALED-UP JENIKE SHEAR CELL

By

Shrey Gupta

August 2009

Chair: Ray A. Bucklin
Major: Agricultural and Biological Engineering

Shear testers such as the Jenike shear cell and the Annular shear cell are used to evaluate flow properties of bulk materials. However, the application of these shear testers is limited by the particle size of the bulk material to be tested. As a consequence, standard shear cells cannot be employed to determine the flow properties of most agricultural grains. In order to effectively evaluate the flow properties large particle sized bulk materials larger shear cells are required. For this purpose, a Jenike shear cell was scaled-up to the size recommended for agricultural grains.

The first objective of the study was to determine whether the flow properties of bulk materials measured by the scaled up Jenike shear cell (SJSC) were equivalent to those measured by a standard Annular shear cell (ASC). Shear tests were performed on wheat flour, cornmeal, mung beans and corn grits to determine their flow properties using both the SJSC and the ASC. The test results showed that in comparison to the ASC, the SJSC gave lower unconfined yield strength values (UYS) for wheat flour but higher UYS values for cornmeal, mung beans and corn grits. A t-test revealed that the flow properties of the four test materials obtained from the SJSC were statistically different (at the 95% confidence interval) from the flow properties obtained through the ASC.

The second objective of this study was to evaluate the efficacy of the SJSC in determining the flow properties of large sized particles. Shear tests were performed on corn and soybeans using the SJSC. The flow functions of soybeans and corn obtained from the SJSC were compared with the flow functions obtained from experimental arching dimension tests on a conical hopper. The comparison revealed that the SJSC estimated significantly higher values of UYS for both corn and soybeans.

Possible factors influencing the measurements of flow properties through the SJSC were investigated. The factors investigated included friction between the steel rods and guides, friction at the base, normal stress inhomogeneity, shear deformation of test material and normal stress variation. Sensitivity analyses on cohesion and angle of internal friction were performed to determine the variation in yield loci so that flow function of the two cells would be identical. Correction factors to correct the flow properties of corn and soybeans were predicted from the sensitivity analysis. Consequently, based on the significant differences between the flow properties of wheat flour, cornmeal, corn grits and mung beans measured on both the SJSC and the ASC, it was concluded that the SJSC was an ineffective tool for shear testing large particle sized bulk solids.

CHAPTER 1
INTRODUCTION

Silos for grain storage and subsequent handling have been constructed for thousands of years. However, an engineering approach to the science of silo construction is less than 150 years old. The main motivation behind the development of engineering methods to design silos can be attributed to the proliferation of agriculture in North America in the later half of the nineteenth century. This event contributed or rather established grain export, as an important and profitable trade. Grain storage became the primary motivation behind constructing silos.

Roberts (1882) was the first to observe that the pressure on the base ceased to increase as depth of grain exceeded about twice the width of the bin. This finding meant that the application of fluid statics principles to estimate pressures in larger bins was no longer acceptable. Janssen (1895) derived an equation for bin pressures, which is still used to predict static and dynamic bin loads. This equation gained acceptance and became to be known as Janssen's equation. Ketchum (1907) modified Janssen's equation by introducing the hydraulic radius (area divided by perimeter of circumference) - adapting the equation to be applicable for bins of any cross section.

The early part of the twentieth century saw developments in the field of bulk solids handling, including studies that addressed the flow of non-cohesive granular type materials from orifices in the bottom of bins and through transfer chutes.

Some of the understanding of the problems in bulk solids handling came from the discipline of soil mechanics. Soil mechanics as a science and an engineering discipline was established in the nineteenth century, and was well understood and widely documented in the first half of the twentieth century. In soil mechanics, while laying a foundation or constructing a retaining wall emphasis is placed on the stress conditions in the soil before failure, whereas in bulk solids handling emphasis is placed on stress conditions in the bulk solid under which failure

and flow occurs. Understanding the flow of bulk solids from a bin or storage vessel in an industry constitutes an important step in reliable handling of bulk solids.

Storage and handling of bulk solids is an important aspect of process industries such as mining, pharmaceutical, chemical, food processing. Powders are often stored in silos, bins and hoppers and removed through an opening in the bottom of the container under the influence of gravity. The reliability of the process involved depends on the flowability of these powders. Free flowing powders do not cause handling problems. However, most powders below 100 μm are cohesive, that is they have tendency agglomerate or stick together over time. This tendency to agglomerate leads to the formation of arches or bridges within the powder mass and must be prevented for the material to flow out of a storage unit. For a stable arch to form, the bulk solid must gain sufficient strength to support itself within the constraints of the container. The cohesive strength is a function of the particle size and the degree of compaction of the material.

Jenike (1961) studied the problems in storage and flow of bulk solids and sought to address the issues concerning design of storage bins and channels for flow. His work gave a new dimension to the understanding of the characteristics of bulk materials and culminated in making the following contributions:

1. Defining two principal flow patterns, Mass-flow and Funnel-Flow
2. Flow/ No-flow criteria of bulk solids form a storage vessel
3. Direct shear apparatus (Jenike shear cell) for the determination of the flow properties of the bulk solids

Jenike's most important contribution was the establishment of appropriate test procedures for the evaluation of flow properties of powders and bulk solids, and thus bolstering the incipient science of Particle Technology.

Jenike was the first to introduce the concept of mechanical continuum to flow of bulk solids, which has been extensively used in soil mechanics. Mechanical continuum theory dictates that the volume element under consideration, composed of a homogeneous material should have negligible body forces, hence the surface forces then alone remain in equilibrium and represent the state of stress in the body at the point being considered. The volume element should be large compared in comparison with particle size. To eliminate the influence of the edges (process boundary wall) on the continuum, the size of the equipment must be large compared to the volume element. As a corollary to the last statement, an argument which questions the feasibility of a shear cell to produce near accurate results for particulate materials of all size range (powders - granular materials) is reasonable. The answer to the argument lies in scaling-up of a shear cell wherein the diameter of the cell relative to volume element (of the largest particle) is large enough to negate edge effects and comply with the theory of continuum mechanics. Hence, to facilitate measurement of flow properties of large sized particles incapable of being measured on a standard shear cell a Jenike type shear cell was scaled-up by a factor of four.

Objectives

The objectives of this study were:

1. To determine whether flow properties of bulk materials measured by the scaled up Jenike shear cell (SJSC) are equivalent to those measured by a standard Annular shear cell (ASC).
2. Based on the flow property comparison between the SJSC and the ASC, determine the efficacy of the SJSC in measuring flow properties of agricultural grains such as soybeans and corn.

CHAPTER 2
LITERATURE REVIEW

A particulate system characterized by properties of the bulk rather than individual particles is regarded as a bulk solid. Chemical powders, agricultural grains, mineral ores, cement, soil etc are examples of bulk solids. Table 1 (Nedderman, 1992; Roberts, 1882) gives a classification scheme based on the average particle size of the system. While powders are prone to agglomeration, segregation in granular mixtures is a major concern. Therefore, depending on solid characteristics, behavioral distinctions can be made allowing material specific design of storage facilities and associated handling equipment.

Particulate systems have traditionally been treated as a continuum. Therefore, rather than the inter-particle forces, the stresses acting on a volume element and the resulting deformation are considered. Assessment of properties of bulk solids at the particle level has become viable by the advances made in Discrete Element Method (DEM) techniques, although the computation power requirement is still colossal and hindering.

Bulk Solid Characteristics

Particle Size

Cohesive strength of a bulk solid is inversely proportional to particle diameter, because inter particle adhesive forces are a function of particle size. Also depending on the particulate system size, increasing fines percentage improves the packing factor of a solid mixture, which adversely increases the unconfined yield strength of the system.

Bulk Density

The ratio of the mass of solid to the total volume (solids + voids). Bulk density is often a function of consolidation pressure. Porosity decreases with increasing consolidation pressure

resulting in a highly compacted bulk solid. Based on the change in porosity when consolidated, a bulk solid can be distinguished as compressible or incompressible solid.

Unconfined Yield Strength

The unconfined yield strength is the major principal stress that would cause an unconfined bulk material to fail in shear at a free interface. Strength of a bulk solid, also known as degree of cohesion, is a consequence of inter-particle adhesive forces. Adhesive forces due to van der Waals forces become important in solids with particle size less than 100 μm. Liquid bridges can form between particles due to high moisture content, consequently exerting a capillary force due to surface tension. Furthermore, other factors such as electrostatic forces, chemical reactions, temperature fluctuations near glass transition temperature, mechanical interlocking of particles can also contribute to strength of a bulk solid.

Commonly, the intensity of an adhesive force increases as inter particle distance decreases or bulk density increases. Therefore, the strength of a bulk solid is regarded as a function of consolidation pressure.

Permeability

Permeability is a measure of resistance to gas flow through a bulk material. It has units of velocity (cm/sec), and can be defined as the superficial velocity (volumetric flow rate/cross-section area) of a gas when the pressure drop across the bulk material due to the gas equals weight per unit area of cross-section of the bulk material. It can then be described as the incipient fluidization velocity. Permeability is substantially affected by porosity changes in bulk materials and hence expressed as a function of bulk density or consolidation stress. Permeability is an important design parameter in determining the limiting flow rate of bulk solids from bins.

Wall Friction

The wall friction is the friction between the solid and a surface such as a bin wall. Knowledge of wall friction angles enables computation of wall loads and hence is a vital parameter in safe bin design and associated bulk solid handling equipment.

Effective Yield Locus

For the flow of bulk materials, there exists a unique relationship between the normal stresses and shear stresses. The collection of all stress states that cause continuous deformation (flow) without volume change can be represented by a linear relationship between shear stress and normal stress as shown in Figure 2-1. A Mohr circle tangent to this line defines a stress state that causes continual deformation without volume change. This line is called the effective yield locus (EYL) and the slope of this line is the effective angle of internal friction (δ).

Storage and Reliable Flow of Bulk Solids

Reliable flow of stored bulk solids is an important unit operation in chemical, mining pharmaceutical, food processing, and grain handling industries. Storage structures called bins - having an upper vertical section and a lower converging section (hopper) - are primarily used as storage facilities for bulk solids. Solids in a bin may experience obstruction to flow as shown in Figure 2-2. An arch forms across a hopper outlet when the solids gain sufficient strength to support their own weight. Stagnant solid regions can form along the bin walls creating a rathole, which effectively reduces the live capacity of the bin.

Jenike (1964) identified two flow patterns in bins:

1. Funnel flow - Solids flow in a channel formed within the solid itself. The solids outside the channel are stationary.
2. Mass flow - The flow channel coincides with the walls of the bin such that the entire solid is in motion whenever any of it is withdrawn.

For mass flow, smooth and steep hoppers are required. Mass flow bins are deployed in industries dealing in powders, involving long storage times and possible segregation issues. Funnel flow occurs in shallow and rough walled hoppers. Funnel flow bins are cheaper to construct as compared to mass flow bins and are common in agricultural and mining industries. Table 2 (Roberts, 1882) summarizes differences between mass flow and funnel flow including advantages and disadvantages.

Design Theory

To predict the conditions required for reliable flow in a bin, Jenike (1964) developed a hopper design theory. Jenike's method of hopper design is unique because it integrates flow theory of particulate solids with flow properties. The theory facilitates computing the critical wall slope (θ) and diameter of hopper outlet (d) for which cohesive arches and ratholes will collapse. The critical diameter of hopper outlet (d) is also known as the arching index.

Description of the theory requires defining the flow function and the flow factor. Flow Factor (ff) is defined by the ratio of major principal pressure (σ_1) acting in the hopper and major principal pressure (fc^*) acting in an obstruction (Equation 2-1). Unconfined yield strength (fc) of a bulk solid is a function of major consolidation pressure ($fc = f(\sigma_1)$). This relation is defined as the flow function (FF) of a solid.

$$ff = \sigma 1 / fc^* \tag{2-1}$$

where ff: flow factor
$\sigma 1$: major principal pressure (Pa)
fc*: unconfined yield strength (Pa)

Jenike introduced a flow-no flow concept. As shown in Figure 2-3, the strength of the bulk solid (represented by flow function: FF) is compared to the stresses acting in the hopper (represented by the flow factor: ff). The point of intersection gives the critical value of fc^*.

Above this value fc^*>fc, implying that any arch will collapse and flow will occur, since stresses in hopper (fc^*) exceed strength of solid (fc). Below this point the stresses acting in the hopper are insufficient to collapse an arch. The intersection point is also indicative of a minimum outlet dimension given by the relationship:

$$d = \frac{fc^*.H(\theta)}{\gamma.g} \tag{2-2}$$

where fc^*: Unconfined yield strength (kPa)
γ: Bulk density of solids (kg/m^3)
H(θ): Geometry factor
g: Acceleration due to gravity (m/s^2)

Flow factors are computed by relating the stresses occurring in the hopper during flow to a radial stress field, both of which satisfy the following functions:

$$\sigma = \gamma.r.s(\theta) \tag{2-3}$$

where γ: Bulk density of solids (kg/m^3)
s(θ): Stress function
r: Length of coordinate ray (m)

$$\omega = \omega(\theta) \tag{2-4}$$

where ω: Angle between the direction of the major pressure and coordinate ray

As shown in Figure 2-4, (θ) is the cone half angle or hopper slope, s(θ) is a stress function and (ω) is the angle between the major principal pressure and the coordinate ray (r). By expressing the component pressures in Figure 2-4 as a function s(θ), two differential equations are obtained. For specific boundary conditions at the hopper, solutions for s(θ) exist and computed. From its definition, flow factor (ff) can be determined from the relation

$$ff = \frac{H(\theta).(1+\sin(\delta)).s(\theta)}{2.\sin(\theta)} \tag{2-5}$$

where δ: Effective angle of friction
H(θ): Geometry factor

s(θ): Stress function

Computed values of flow factors as a function of hopper slope (θ) and kinematic angle of friction between wall and solid (ϕ_x), for specific values of effective angle of friction (δ) are presented by Jenike (1964) in a series of charts for axisymmetric and plane flow hoppers. The graphs exhibit contours of constant value flow factors. Solutions for s(θ) exist only for specific combinations of (δ, ϕ', θ), beyond which radial stress field assumption fails and material ceases to flow along the walls, resulting in funnel flow.

Jenike Shear Cell

Apparent from the above discussion is the need for quantification of flow properties of bulk solids. This is facilitated by a translation shear tester developed by Jenike and Johanson (Jenike, 1964) called the Jenike shear cell. As shown in Figure 2-5 (ASTM, 1997), the standard shear cell consists of 2 concentric rings with an inner diameter of 95mm and thickness 3mm. The height of the base (1) is 13 mm and that of the shear ring (3) is 16 mm. The base (1) is closed at its lower end and fixed on the base plate (2) of the apparatus. The shear ring (3) is positioned on top of the base, and can move horizontally up to 6mm. The bulk solid is filled in the cell and covered by a shear lid (4). A weight hangar system is used to apply a normal force (N) transmitted centrally to the bulk solid through the lid (5). The shear force (S) is applied via a bracket (6) to the shear lid (4) and via the shear pin (7) to the shear ring (3). The shear force which is applied using a motor driven shear stem (8) is measured by a force transducer and recorded.

To run a shear test, the cell is filled with a representative sample of material and pre-consolidated by means of normal force (N) applied centrally on the lid. The lid is then twisted. Upon pre-consolidation the sample is sheared in two steps. First, the pre-shear step, in which

shearing continues until steady state flow develops. This state is marked by constant shear stress (τ_p) at the specified normal stress (σ_p). The shear stem is then retracted and load decreased.

Preshear yields a homogeneous state of material with regard to bulk density and material strength. This state is reproducible, hence it can be repeatedly sheared to failure under decreasing normal load values. In the shear step, the critically consolidated sample is sheared again until a peak shear stress (τ_s) is recorded. This peak stress is indicative of incipient failure of solid under normal stress (σ_s) and yields a point on the yield locus.

Yield Locus

Repetition of the test with freshly prepared samples at constant normal loads during preshear and varying normal loads during shear yields additional shear points that can be represented on a shear stress- normal stress diagram according to the relationship

$$\tau = \sigma.\tan(\phi) + c \tag{2-6}$$

where τ: Shear stress (kPa)
σ: Normal stress (kPa)
ϕ: Angle of internal friction (degrees)
c: Cohesion (kPa)

The yield locus represents the bounding curve or line that describes the stress states that will produce failure of a consolidated and pre-sheared bulk material. As illustrated in Figure 2-6, a Mohr stress circle constructed through the pre-shear point (σ_p, τ_p) and tangent to the yield locus, defines the major principal stress (σ_1) acting during steady state flow. Another Mohr stress circle, drawn through the origin, defines the unconfined yield strength (fc). There is one yield locus for each consolidation stress and one value of unconfined yield strength for each major principal stress. In addition, a straight line through the origin tangent to the yield locus is defined as the Effective yield locus (EYL). From the definition of yield locus all the flow properties of a bulk material can be evaluated using Equation 2-7 to Equation 2-10.

$$\sigma 1 = \frac{-[\sigma_s + c.\cos(\phi) - \sqrt{(c^2.\cos^2(\phi) + \sigma_s{}^2.\sin^2(\phi) + \tau_s{}^2.\sin^2(\phi) + 2.\sin(\phi).\sigma_s.c.\cos(\phi) - \tau_s{}^2)}]}{(\sin(\phi) - 1)} \tag{2-7}$$

$$\sigma 2 = \frac{(1 - \sin(\phi))}{(1 + \sin(\phi))}.\sigma 1 - 2\left(\frac{c.os(\phi)}{(1 + \sin(\phi)}\right) \tag{2-8}$$

$$fc = \frac{2.c}{(1 - \sin(\phi))}.\cos(\phi) \tag{2-9}$$

$$\delta = \sin^{-1}\left(\frac{(\sigma 1 - \sigma 2)}{(\sigma 1 + \sigma 2)}\right) \tag{2-10}$$

where σ1: major principal stress (kPa)
σ2: minor principal stress (kPa)
c: intercept of yield locus with y-axis (kPa)
ϕ: angle of internal friction (degrees)
δ: effective angle of internal friction (degrees)
fc: unconfined yield strength (kPa)

Wall Yield Locus

Replacing the base with a sample of the wall material as shown in Figure 2-7, facilitates measurement of the wall friction angle. After the modification is made, in a single test run, the sample is sheared continuously and the shear force (F_S) recorded until a steady state condition prevails for every step-wise decrease in normal force (F_N). The locus of the corresponding wall shear points presented on a shear stress – normal stress diagram is called the wall yield locus. The locus can be a straight line, indicating a constant wall friction angle or a curved line indicating a wall friction angle depended on the normal stress level. Wall friction angle (ϕ_x) is given by the relation

$$\tan(\phi_x) = \frac{F_S}{F_N} \tag{2-11}$$

where F_S: shear force (N)
F_N: normal force (N)

The Jenike shear cell has been the most widely used shear tester for over 40 years, but other types of shear testers have been also been developed to serve the same purpose.

Johanson Hang-Up indicizer

In the Johanson Hang – up indicizer, a cylindrical bulk solid specimen is compressed in the axial direction (force F_u) via an upper piston consisting of two concentric areas as shown in Figure 2-8. After consolidation, the piston at the bottom of the specimen is removed along with the outer ring of the top lid. The powder is then loaded with the inner piston until failure. From failure force (F_f), the unconfined yield strength (f_c) can be calculated. However, internal friction angle (ϕ), and effective angle of internal friction (δ) cannot be evaluated.

Schulze Shear Tester

A type of annular shear cell known as the Schulze shear tester is shown in Figure 2-9. For running a shear test, a representative sample of the bulk solid is filled in the bottom ring and covered with a annular lid on top. A normal force (F_N) is transmitted to the bulk solid by means of a weight hangar. Shearing is induced by rotating the bottom ring with angular velocity (ω), while holding the annular lid stationary by means of a cross-beam. The torque acting on the annular lid is measured as sum of the forces ($F_1 + F_2$) acting on the tie rods. The bulk solid is sheared until steady state flow is achieved, denoted by constant shear stress conditions. After Normal force (F_N) is reduced and shearing is re-initiated until a peak shear stress is recorded, giving a point on the yield locus.

Since, rotation provides unlimited shear strain, the Schulze shear tester can more accurately evaluate flow properties of soft elastic solids like plastic powders, rubber granules and plastic materials like filter cake, plastic clay, and sewage sludge. Also, due to unlimited strain, shear tests can be repeated without having to refill the cell.

Bin Loads

The horizontal and vertical pressures in stored solids impose loads on bins. These pressures are of significant interest not only from the design perspective but also due to safety concerns. Collapse of an improperly designed bin is not uncommon and can produce tremendous economic and safety issues on the particular industry.

Janssen (1895) found that significant wall loading occurred due to the friction between the bulk solid and bin walls. Eventually researchers established that initial loading conditions exist during charging and that different flow loading conditions exist during discharge of solids from a bin. These conditions differ in the stress fields that are set-up in the bin. In addition, switch loading occurs during transition from initial to flow loading. Switch loading is transient, but imposes a large concentrated force on the bin.

Static and Dynamic Stress Fields

During initial loading with the hopper gate closed, bulk solids are compressed vertically with very little horizontal deformation. As shown in Figure 2-10, the major principal pressures are aligned vertically, which implies that an active stress state or a static stress field exists in the bin. When the hopper outlet is opened, and flow starts, the bulk solids form a flow channel that converges downward towards the outlet. In the flow channel, bulk solids expand in the vertical direction while contracting in the lateral direction. The major principle pressures align in the horizontal direction (Figure 2-10), which implies that a passive stress state or a dynamic stress field exists in the bin.

Switch

A static stress state field exists in a completely filled bin, but for flow, a dynamic stress field exists. Thus, when a hopper gate is opened, and assuming the solid flows freely without forming arches, a switch in the stress field occurs near the hopper bottom and travels upward in

the bin. Figure 2-11 illustrates a switch stress state and associated vertical stress (σ_v) and wall stress (σ_w) profiles. Above the switch a static stress filed exists and below a dynamic stress field prevails. The switch produces a concentrated force on the bin wall.

For estimating switch loading on the walls in mass flow bins, Walters (1973) proposed a ratio of dynamic to static stress times static wall stress at switch height Z. Jenike and Johanson (1969) noted that one of the requirements for development of mass flow in a bin is that pressure exerted by the solids in the vertical section of the bin on solids in the hopper must be equal to or greater than the radial pressures in the hopper. Therefore a minimum surcharge is required at the transition to enable mass flow. If the minimum surcharge is attained with a passive stress field, the switch travels upward in the bin. But in case of an active stress field in the vertical section the switch gets arrested at the transition.

Stresses in Vertical Section

Assuming the horizontal bin wall stress (σ_h) to be equal to a constant (k) times vertical stresses (σ_v) (Equation 2-12) at any given height in the bin, a vertical force balance (Figure 2-12) on a horizontal material slice of thickness (dh) and cross-sectional area (A) can be evaluated. Such an analysis yields a differential equation (Equation 2-13) for vertical stress in a cylindrical channel.

$$\sigma_h = K.\sigma_v \tag{2-12}$$

$$\frac{d\sigma_h}{dh} + \sigma_v.K.\frac{U}{A}.\tan\phi' = \gamma.g \tag{2-13}$$

$$\sigma_v = \frac{g.\gamma.A}{K.\tan\phi_x.U}\left(1 - \exp\left[-\frac{-K.U.\tan\phi'.h}{A}\right]\right) \tag{2-14}$$

where γ: Bulk density of solids (kg/m^3)
g: Acceleration due to gravity (m/s$^{2)}$
ϕ': Kinematic friction angle between wall and solid (degrees)
U: Circumference of bin (m)

Integrating Equation 2-13 over the entire height of the vertical section yields Janssen's equation (Equation 2-14). It is used to compute static loads in bins and is modified by overpressure factors to estimate dynamic loads. This analysis requires selecting a K value. However, the proper method for choosing an appropriate value for K has been widely speculated in the literature. Jenike, et al. (1973) suggested a global value of K = 0.4 for granular materials, whereas Walker (1966) described K as a function of wall friction angle (ϕ') and effective angle of friction (δ). In addition, K has been proposed to be similar to Rankine coefficient (Schulze, 2008)(Equation 2-15) in soil mechanics. It should be noted that application of Equation 2-15 in combination with Janssen's equation implies that the vertical and horizontal stresses in the vertical section are principal stresses (which due to presence of wall friction is only possible along the axis of the vertical section).

$$K = \frac{\sigma_2}{\sigma_1} = \frac{1-\sin(\delta)}{1+\sin(\delta)} \tag{2-15}$$

where σ_1 and σ_2: Major and minor principal stresses respectively (kPa)
δ: Effective angle of internal friction (degrees)

Stresses in Hopper

Walker (1966) and Walters (1973) extended Janssen's element slice technique to determine stresses in hoppers. Walker used a rectangular element slice, while Walters used frustum of a cone which is more conforming element slice. As shown in Figure 2-13, a force balance on a differential element slice of thickness (dz) and cross-sectional area (A) is defined. Resolution of forces in the vertical direction yields Equation 2-16.

$$\gamma.g = \frac{1}{A}.\frac{dA}{dz}.\sigma_v + \frac{d\sigma_v}{dz} + (\tau_w + \sigma_h.\tan\theta).\frac{P}{A} \tag{2-16}$$

where τ_w: shear stress along the wall (kPa)
θ: cone half angle (degrees)
P: perimeter at depth Z (m)

Depending upon the stress field in the hopper, Equation 2-16 can be solved by establishing a relationship between vertical stress (σ_v) and horizontal wall stress (σ_h). Estimates of K are based on engineering experience in designing storage systems. As a consequence, no single unifying technique for computing K can be found in the literature.

Jenike, et al. (1973) pointed out that in commercial bins, the presence of local surface imperfections is inevitable. During mass flow, these local convergences control the formation of wall boundary layers of solids, and thus determine the nature of the prevailing stress field. For perfectly straight walls with no surface irregularities, wall boundary layers are absent and the initial Janssen stress field prevails. Where boundary layers exist, flow pressures are predicted by assuming that the elastic strain energy within the flowing mass tends towards a minimum.

The changes between the stress fields initiated by local convergences in the cylinder occur as a switch at some depth, h, in the channel. Therefore, the initial Janssen pressure field applies between the top of the cylinder and the switch. Below this level, between the switch and level of free boundary condition the minimum strain energy applies. However, due to the random nature of such surface irregularities, it is difficult to predict the exact location of the switch and the consequential overpressure peak in advance. Moreover, Jenike, et al. (1973) point out that such a switch in the stress field is unstable and reverts back to its original form some distance away form the local disturbance causing it.

Bilgili, et al. (2004) investigated possible normal stress inhomogeniety in a powder specimen tested in a Jenike shear cell via. shear experiments and Discrete Element Method

(DEM) simulations. They performed shear tests using a standard Jenike cell fitted with a pressure sensing TekScan pad along the bottom of the cell which facilitated measurement of normal stress at the bottom section of the cell. The normal stress profiles pertaining to pre-shear and shear to failure indicated significant spatiotemporal variation in the stress field, with substantial redistribution of normal stress along the leading edge. The normal stress decreased from the mid-section of the cell towards the cell walls with shearing at the bottom of the cell. The variation was attributed to the variation in both magnitude and direction of the principal stresses with respect to position in the cell. This experimental evidence suggested that the Jenike shear cell and test method do not produce uniform stress, at least along the bottom surface of the cell during operation. Furthermore, by simulating the contact force pattern using Discrete Element Method (DEM) techniques, the experimental observation of existence of an inhomogeneous stress field along the base was qualitatively validated. But, more importantly, using DEM simulations the nature of the normal stress field in the shear zone was predicted. The contact force pattern illustrated preferential alignment of the force chains towards the leading edge along the bottom of the cell with shearing. Thus normal stress in the shear zone exhibited fluctuations similar to the type simulated along the base. DEM simulations also corroborated spatial variations of the principal stresses and their directions.

Table 2-1. Classification of Bulk Solids

Classification	Particle size range (µm)
Ultra-fine powder	<1
Superfine powder	1-10
Granular powder	10-100
Granular solid	100-300
Broken solid	>3000

Table 2-2. Comparison of mass flow and funnel flow

Comparison criterion	Mass flow	Funnel flow
Characteristics	No stagnant zones Uses full cross-section of the vessel First-in, first-out flow	Stagnant zone formation Flow occurs within a portion of vessel cross-section First-in, last-out flow
Advantages	Often minimizes segregation, agglomeration of materials during discharge	Small stresses on vessel walls during flow due to the “buffer effect” of stagnant zones. Very low particle velocities close to vessel walls, reduced particle attrition and wall shear
Disadvantages	Large stresses on vessel walls during flow Attrition of particles and erosion and wear of vessel wall surface due to high particle velocities Small storage volume/vessel height ratio	Promotes segregation and agglomeration during flow Discharge rate less predictable as flow region boundary can alter with time

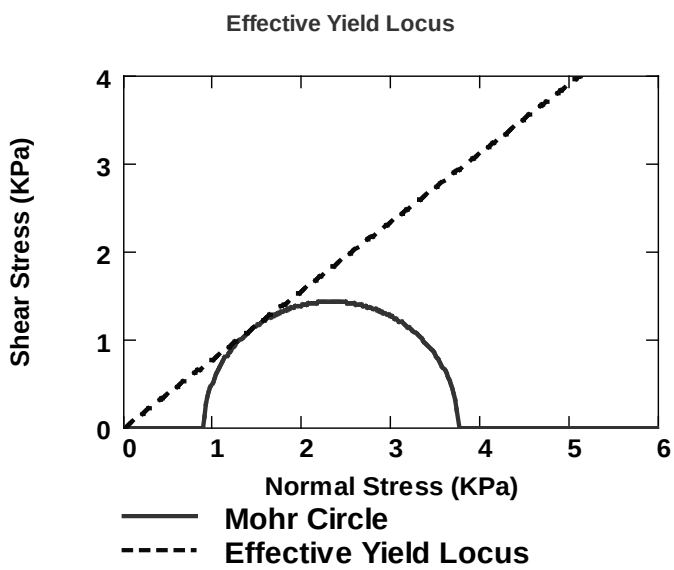

Figure 2-1. Effective yield locus

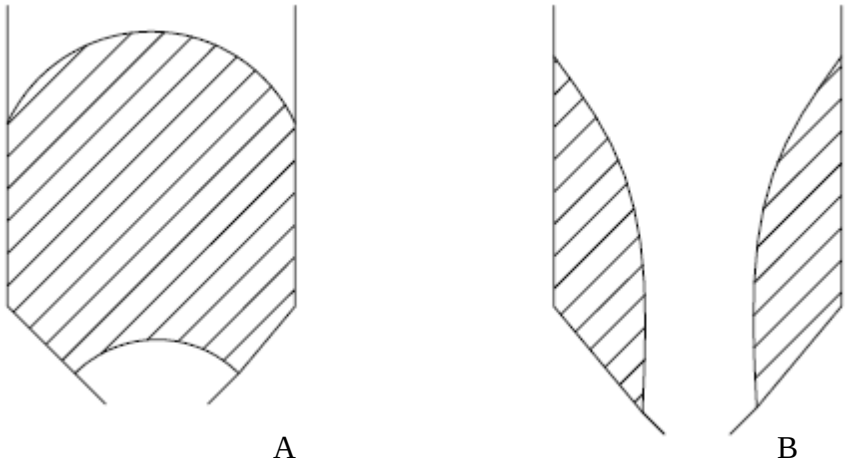

Figure 2-2. Orientation of major principal stresses. A) Initial loading. B) Flow loading

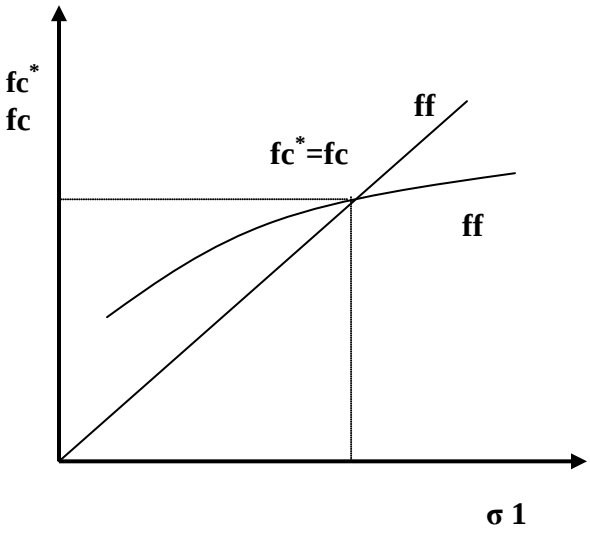

Figure 2-3. Flow-no flow concept for mass flow hopper design

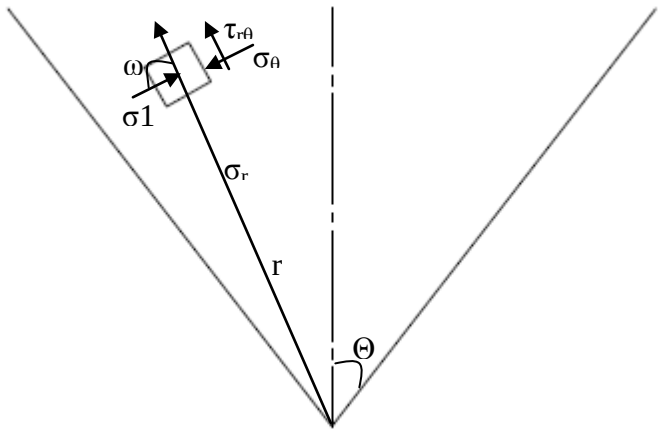

Figure 2-4. Polar coordinates in a hopper

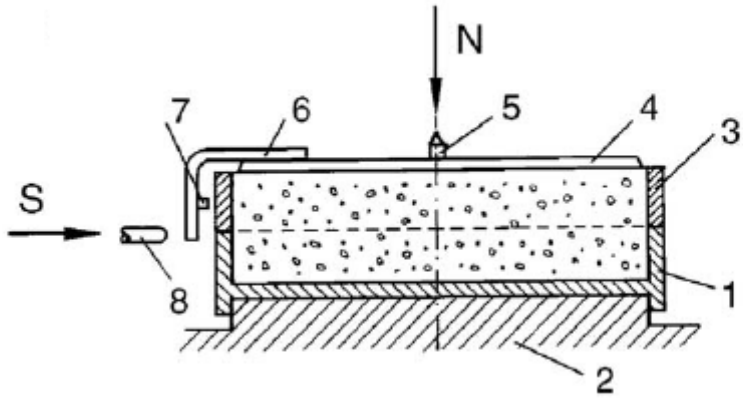

Figure 2-5. Jenike shear cell

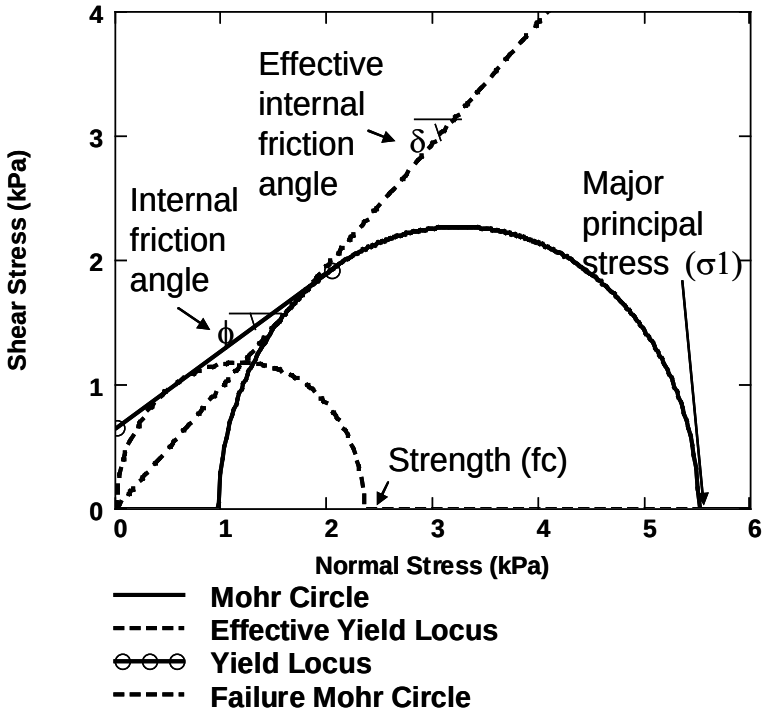

Figure 2-6. Typical yield locus

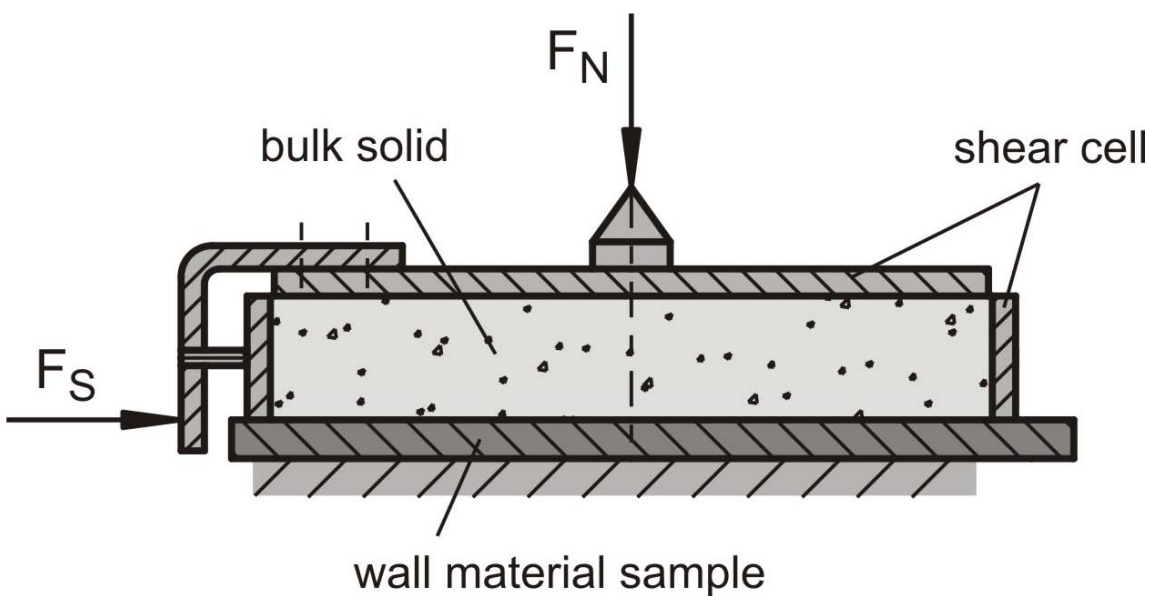

Figure 2-7. Jenike shear cell set-up for wall friction test

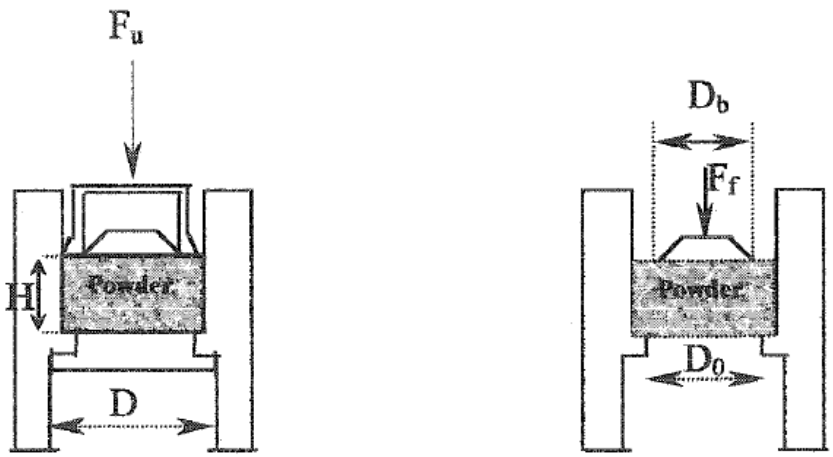

Figure 2-8. Johanson Hang-up indicizer

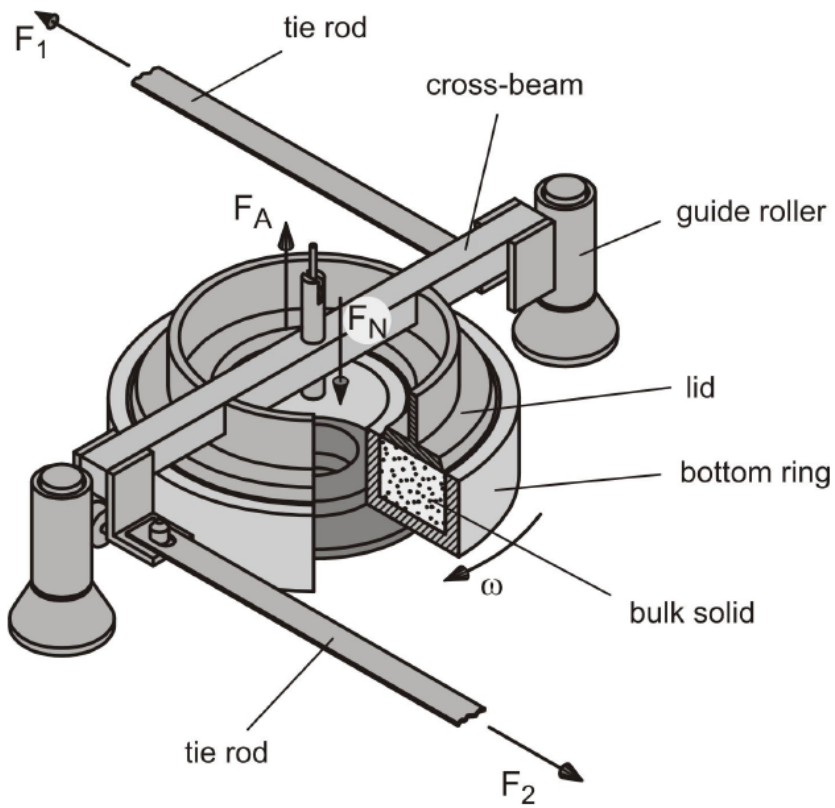

Figure 2-9. Schulze shear cell

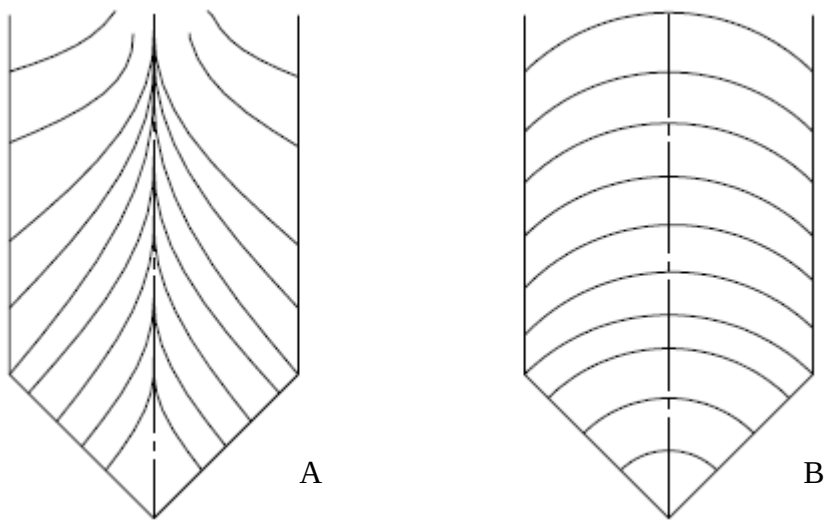

Figure 2-10. Orientation of major principal stresses. A) Initial loading. B) Flow loading

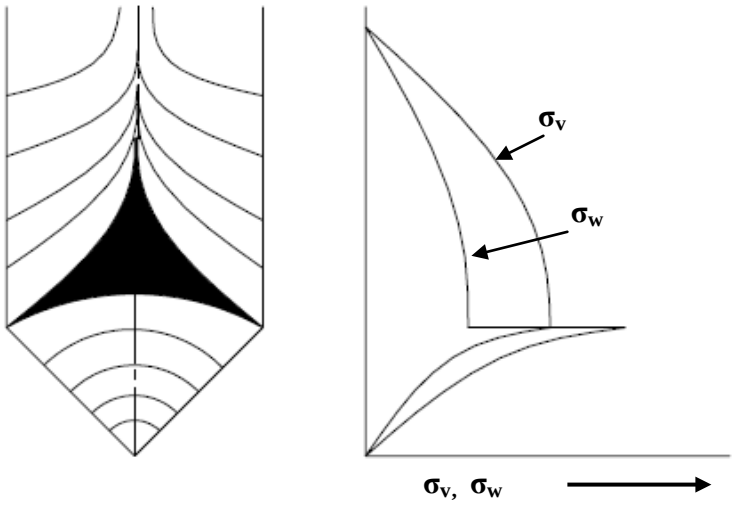

Figure 2-11. Orientation of major principal stresses during switch stress

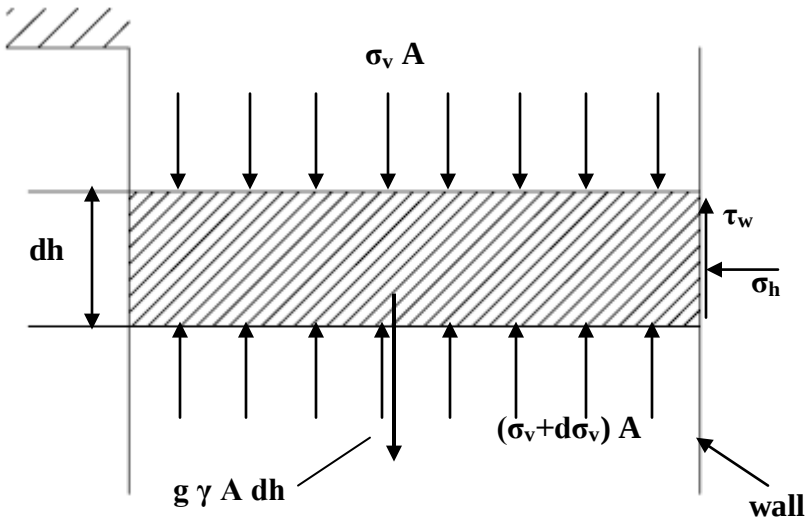

Figure 2-12. Forces acting on a horizontal material slice

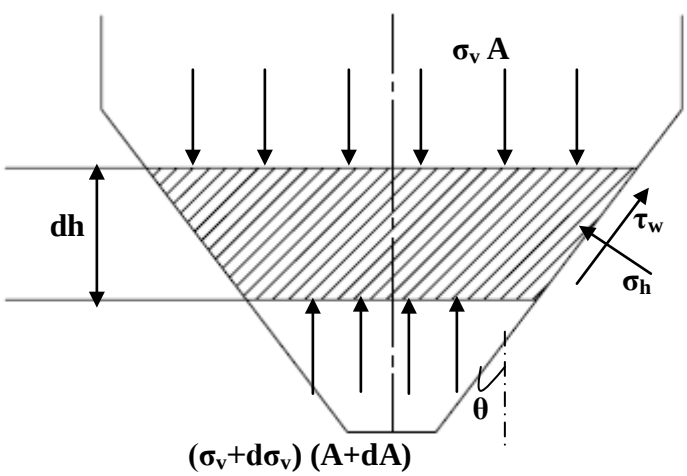

Figure 2-13. Differential element slice of a hopper

CHAPTER 3
MATERIALS AND METHODS

In this study, shear tests were performed on wheat flour, cornmeal, corn grits, mung beans corn and soybeans to determine their flow properties using the annular shear cell (ASC) and an experimental scaled-up Jenike shear cell (SJSC).

Wheat flour, cornmeal, corn grits, mung beans, corn and soybean were selected for use as test materials for several reasons. They are inexpensive, readily available and are of great importance to the food industry. Also, soybean and corn are important economic commodities due to their increased use as raw materials for ethanol production.

Physical Property Measurement

Bulk Density

The test material was poured into a 1000 ml graduated cylinder up to the 1000 ml mark. To ensure uniform fill, the cylinder was tapped three times on a flat surface and weighed. The bulk density was then computed as the ratio between mass of the test material and its volume (1000 ml). This procedure was repeated thrice and the average reported as the bulk density.

Moisture Content

Moisture content (wet basis) of the test materials was found by the oven dry method (ASAE, 2003). Test material samples each weighing 5 grams were placed in moisture dishes. The moisture dishes were then placed in an oven at 103°C for 72 hours. At the end of the heating period the dishes were removed and weighed immediately. The moisture content was calculated as loss in moisture during heating divided by weight of the original sample.

Geometric Mean Diameter

The geometric mean diameter is defined as the cube root of product of the three principal axes (Mohsenin, 1986) was determined by measuring the three principal dimensions of mung beans, corn and soybean using a shadowgraph.

Mean Particle Pize

Particle size distribution for cornmeal, wheat flour and corn grits was determined using a laser diffraction particle size analyzer (Beckman, 2005).

Choice of ASC over Jenike Shear Cell

Schwedes (2003) identified two important limitations of the Jenike shear cell.

1. The Jenike shear cell requires a high level of training and skill
2. The maximum strain in the Jenike shear cell is small and sometimes not sufficient

The ASC overcomes both these limitations. Comparative studies presented by Schwedes (2003) show good agreement between the results gained with the Jenike shear cell and ASC. As a result ASC was chosen over the standard Jenike shear cell in the current study.

Annular Shear Cell (ASC)

The ASC, shown in Figure 3-1 to 3-2 is composed of a base (1) and casing (2). The casing contained the driving and measuring units. The shear cell (3) had an internal diameter of 60 mm and outside diameter of 120 mm and was provided with driver pins at its underside, which rested in the toothed wheel of the driving axle (4). The driving axle was rotated by an electric motor, which could cause the shear cell to rotate to the right or to the left. The shear cell lid (5) as well as the bottom of the shear cell had bent bars to prevent slipping of the test material at the lid or the bottom of the shear cell. The crossbeam (6) was fixed to the shear lid. At its center was a hook to append the weight hangar (7). Bolts at the end of the crossbeam were used to append the tie rods (8). The opposite end of the tie rods connected to the load beam (9). The rotation of the

lid was prevented by the tie rods which transferred the tensile force to the load beams. A hook suspended from the balance arm (10) was attached to the crossbeam so that the shear lid floated just over the shear cell. The balance arm along with the counterweight (11) served to compensate the weights of the shear lid, crossbeam, hangar and the tie rods. Shear tests were performed in accordance with the ASTM Standard D 6773 (ASTM, 2008)

Calibration

One of the guide rollers was removed and positioned in the calibration configuration on the end of the apparatus. The chart recorder was started. The weight trolley was suspended on the guide roller and its hook was connected to the load beam. The response of the chart recorder due to weight of the trolley (180 g) was observed and upon equilibration the response was labeled. A 2 kg weight was added to the weight trolley and chart recorder was observed for steady response. The steady response was labeled appropriately and procedure repeated with another 2 kg weight piece. A digital micrometer was used to measure the height of the calibration response on the chart recorder. A calibration plot of weight versus height response was constructed. Using linear regression, a straight line was fitted to the data points and the equation of the regression line served as the calibration equation.

Filling the Cell

The shear cell was filled uniformly with the test material in small horizontal layers by a spatula until the material was somewhat over the top of the cell wall. Excess material was struck using a blade, to yield a leveled surface flush with the shear cell.

Pre-shear

The filled shear cell was secured on the driving axle. The shear lid was then connected to the balance arm through the hook and weight hangar with a weight piece was appended to the lower side of the crossbeam. The shear lid was then carefully placed concentrically on the shear

cell on the test material. The tie rods connected to the load beams on one end were then connected to the shear lid.

Weight (m_p) corresponding to a pre-shear normal stress (σ_p) was placed on the hangar and the motor started and shear force (F_p) monitored. As soon as the shear force (F_p) attained a constant value indicated by a near – constant response on the chart recorder, the direction of rotation was reversed, until the tie rods had a clearance of 2 mm with the load beams. The shear force (F_p) corresponded to a pre-shear shear stress (τ_p).

Shear

The weight on the hangar was replaced by a smaller weight m_s corresponding to a shear normal stress (σ_s). The motor was switched on in the forward direction and the material was sheared until the shear force went through a maximum representing the failure shear stress (τ_s) and then began to decrease. The values of (σ_s,τ_s) corresponded to a single point on the yield locus. The shear tests were repeated with shear normal stress (σ_s) values between 25% - 80% of the pre-shear normal stress (σ_p) to obtain 5 – 6 shear points.

The shear tests were repeated for four different pre-shear normal stress values to obtain four points on the flow function.

Data Processing

A software application (PTC, 2007) was created for data processing. It carried out the following steps.

Normal stress calculation

Normal force (F_N), (given by product of mass of the weight pieces and acceleration due to gravity) was divided by the cross-sectional area of the tester.

$$A = \frac{\pi}{4}(D_{out}^2 - D_{in}^2) \tag{3-1}$$

$$\sigma = \frac{F_N}{A} \tag{3-2}$$

where D_{out} and D_{in}: outside and inside diameter of the tester (m)
$F_{N:}$ normal force (N)

Shear stress calculation

The heights of the preshear and shear points were measured using a digital micrometer and the calibration plot was used to convert the height response into corresponding shear force values (F_S).

The shear stress was calculated from equilibrium of moments (moment due to shear force F_S and moment due to shear stress τ).

Moment M_d due to shear force is

$$M_d = r_s F_S \tag{3-3}$$

Moment arm r_m of force τ.A is

$$r_m = \frac{2}{3}\frac{(r_{out}^3 - r_{in}^3)}{(r_{out}^2 - r_{in}^2)} \tag{3-4}$$

Mean shear stress τ acting on the bulk solid is

$$\tau = \frac{M_d}{r_m A} \tag{3-5}$$

where r_s: moment arm distance to load beams (0.125 m)
F_S: shear force calculated form calibration equation (N)
r_{out}, r_{in}: outer and inner radius of the lid (m)

Prorating

All of the measured shear stress (τ_s) values were prorated to account for the scatter between the pre-shear shear stresses (τ_p) for a given pre-shear normal stress (τ_p). Prorated values of (τ'_s) were calculated using the equation.

$$\tau'_s = \tau_s \frac{\bar{\tau}_p}{\tau_p} \tag{3-6}$$

where τ_p: pre-shear shear stress for a specific pre-shear normal stress level (kPa)
τ_s: measured shear stress corresponding to τ_p (kPa)
$\bar{\tau}_p$ **:** average of the pre-shear shear stresses τ_p for a specific normal stress level (kPa)

The yield locus was obtained by plotting the prorated shear stress values (τ'_s) versus the corresponding shear normal stress (σ_s) values for a particular pre-shear normal stress (σ_p) and a straight line was fitted to the points using linear regression. The average pre-shear stress value ($\bar{\tau}_p$) for the pre-shear normal stress (σ_p) was then plotted on the graph and if it fell above the regression line, the regression model was changed so that the yield locus passed through the pre-shear stress point (σ_p, $\bar{\tau}_p$). The slope of the yield locus was equal to the angle of internal friction of the test material for the corresponding pre-shear consolidation stress. The unconfined yield strength, major principal stress and effective angle of internal friction were calculated using Equation 2-3 to 2-6 respectively.

Scaled-up Jenike Shear Cell (SJSC)

The SJSC, shown in Figure 3-3 and 3-4 consisted of a 50 mm thick base plate (1) made from magnesium. At its center, a cylindrical cavity with a diameter of 380 mm extended up to 38 mm into the base plate. The hollow cavity served as the base of the SJSC. The shear ring (2), constructed from magnesium, had an internal diameter of 380 mm, and was 38 mm in height and 28 mm thick. The shear ring rested on the base plate over 2 Teflon strips (3) and could travel a shear distance of 56 mm. The Teflon strips served to reduce friction between the shear ring and base plate.

Two steel rods (4) were attached to the shear ring. The steel rods were supported on four Teflon guides (5) which were secured to the base plate. The Teflon guides served the purpose of limiting the shear ring's motion to translation. The steel rods terminated in a crossbeam (6). At

the center of the crossbeam a cable fastener was provided to which a steel cable was fastened. The other end of the steel cable was connected to the crosshead of an Instron universal testing machine (7) through a pulley system. The Instron measured the horizontal (shear) force required to pull the shear ring at a constant rate of 13 mm/min.

Due to the large size of the SJSC, very high normal forces were required to perform shear tests. For example, to perform a shear test under pre-shear normal stress of 6 kPa, a normal force of 325 N was required. As a result, the SJSC was equipped with a rectangular loading frame (8) attached to a pneumatic cylinder. The loading frame could be placed centrally on the shear lid (9) to facilitate uniform loading of the test material. Pressure from the pneumatic cylinder was controlled using a pressure gauge (10). The shear lid could be loaded with a maximum force of 1538 N (12 kPa).

The SJSC was fitted with 2 sets of 4 equally spaced vanes (11) with one set in the base and the other in the shear ring. The distance between the 2 set of vanes was approximately 7 mm, enough to allow unhindered formation of the shear zone. The vanes served to reduce the normal stress inhomogeneity occurring in the SJSC, which was manifested by the tilting of the shear lid during shear tests.

Due to the high normal loads acting on the shear lid, twisting was realized by using a special apparatus. The SJSC consisted of a vertical shaft (13) which was connected to an electric motor (14) at one end and a 3-piece crank (12) on the other end. The 3-piece crank connected to a twisting arm (15) positioned over the offset shear ring. The shaft was rotated by a vertically placed electric motor and the 3-piece crank turned the rotation motion of the shaft to a 90° reciprocating motion in the twisting arm. The shear lid and the twisting arm were provided with two coincident perforations, through which 2 cylindrical rods could be inserted and wedged. The

rods helped transmit the torque from the twisting arm to the twisting lid, and thus imparted the twisting motion to the lid.

The procedure for running a shear test on the SJSC comprised of four steps.

Filling the Cell

With the shear ring in an offset position over the base, small scoops of the test material were deposited in the cell. The cell was filled until the material was somewhat over the top of the shear ring.

Preconsolidation

The shear lid was placed on the test material surface and the loading frame was placed on the shearing lid. The pressure gauge was adjusted to apply a normal force (F_N) which corresponded to a normal pre-shear stress (σ_p). For the test material, wheat flour and cornmeal the material was compressed. After the vertical movement of the shear lid stopped the cell was refilled and loaded. The refilling was repeated until no further material compression occurred. The test materials were twisted through 20 cycles. .

Pre-shear

After twisting, the rods connecting the twisting arm and the shear lid were removed. The shear lid was loaded with a normal force (F_P) which corresponded to a normal pre-shear stress (σ_p). The Instron machine was started to initialize the shearing action. The shear force was recorded until the shear stress reached a constant value (F_P) which corresponded to a steady pre-shear shear stress (τ_p). The parameters (σ_p,τ_p) yielded the pre-shear point for a specific consolidation stress on the yield locus.

Due to large shear distance (57 mm), it was anticipated that any inhomogeniety in the test material would be compensated after sufficient shear deformation. Thus an over-consolidated or

under-consolidated sample was sheared until constant shear stress was recorded. The test materials were pre-sheared under normal stress values of 6, 8, 10 and 12 kPa.

Shear

After pre-shear, the pressure was adjusted to load the test material with a smaller normal force (F_S) corresponding to a shear normal stress (σ_s). The Instron machine was started and the shear force recorded until it passed through a maximum (F_S) and then began to decrease. The maximum shear force (F_S) corresponded to a failure shear stress (τ_s). The values of (σ_s,τ_s) corresponded to a single point on the yield locus. The shear tests were repeated with shear normal stress (σ_s) values between 25% - 80% of the preshear normal stress (σ_p) to obtain 5 – 6 shear points.

Data Processing

A software application (PTC, 2007) was created for data processing. It comprised of the following steps.

Normal stress calculation

Normal force (F_N), (given by product of the pressure gauge reading and the force factor of the pneumatic cylinder) was divided by the cross-sectional area of the tester.

$$\sigma = \frac{F_N}{A} \tag{3-7}$$

where A: cross-sectional area of the tester (m^2)
F_N: normal force (N)

Shear stress calculation

Shear force obtained from the computer interface of the Instron machine was divided by the cross-sectional area of the tester.

$$\tau = \frac{F_S}{A} \tag{3-8}$$

where F_S: shear force (N)
A: cross-sectional area of the tester (m^2)

To obtain yield locus and the corresponding flow properties steps similar to that of the ASC were followed.

Measurement of Kinematic Wall Friction

A friction box apparatus (Mohsenin 1986) was used to measure the kinematic friction of mung beans. Wall friction tests were performed on cornmeal, corn grits and wheat flour using the standard Jenike shear cell (ASTM, 1997). The base of the shear cell was replaced with a clean flat plate of aluminum (wall coupon). The shear ring having an inner diameter of 95mm and thickness 3mm was placed on the wall coupon and set against the locating screws. The mould ring was placed over the shear ring and the space between them filled with the test material. Excess material was scraped flush with the mould ring.

Consolidation

The twisting lid was placed over the test material along with the weight hanger placed on the twisting lid. Weights (F_N) corresponding to the largest normal stress (σ_w) of the intended wall friction test were placed on the hangar. The lid was then twisted several times by means of twisting wrench to homogenize the test material.

Wall Shear

After twisting, the weight hangar was removed and twisting lid replaced with the shear lid. The weight hangar was placed on the shear lid and weights corresponding to the highest wall normal stress (σ_w) were placed on the weight hangar and the motor driving the force measuring stem was started. The test material moved relative to the wall surface and shear force (τ_w) began to rise and attained a constant value (Figure. 3-5). The normal stress (σ_w) was then reduced and

the shear stress (τ_w) again monitored to obtain a corresponding constant value. This procedure was repeated to obtain 4 wall shear points.

The wall normal stresses and wall shear stresses were plotted in shear stress – normal stress space and a straight line was fitted to the points using linear regression to obtain the wall yield locus. If the wall yield locus does not pass through the origin, then slope of the lines through individual wall shear points and the origin was found and reported as the wall friction angle (ϕ_x).

Measurement of Unconfined Yield Strength Using a Conical Hopper

A conical hopper made from mild steel was used to experimentally measure the unconfined yield strength of corn and soybean using the following relationship.

$$d = \frac{fc^{*}.H(\theta)}{\gamma.g} \tag{3-9}$$

where d: critical diameter of hopper outlet (m)
fc^*: unconfined yield strength of the solid in the arch (obstruction) (Pa)
γ: bulk density of solids
$H(\theta)$: geometry factor
g: acceleration due to gravity (ms^{-2})

The hopper had a conical half angle of 31° and a height of 2 ft. The diameter of the outlet of the hopper was varied by placing transparent plastic funnels of fixed opening size at the bottom of the hopper. The plastic funnels were chosen such that arching occurred when test material was filled in the hopper. Upon filling, a marking was made at the arching level and the hopper emptied. The diameter of the funnel at the marking was equal to the arching index of the test material. The arching index of corn and soybean was 33 and 19 mm respectively. From equation 3-3 the unconfined yield strength (fc^*) of the test material in the arch was calculated. Equation 3-4 gives the normal stress (σ_{out}) acting at the hopper outlet. Thereby a single point (σ_{out},fc^*) was experimentally obtained on the flow function of test materials corn and soybean..

$$\sigma_{out} = 0.5.\gamma.g.d \tag{3-10}$$

where σ_{out}: normal stress acting at the hopper outlet (Pa)
γ: bulk density of solids (kg/m^3)
g: acceleration due to gravity (m/s^2)
d: critical diameter of hopper outlet (m)

For both corn and soybean, a straight line having a slope equal to the slope of the flow function obtained from the SJSC was fitted through the experimental point (σ_{out},fc*). This method gives a crude estimate of corn and soybean flow functions and was useful for making comparative assessments.

The difference between the flow functions obtained from the SJSC and hopper test at a pre-shear consolidation stress of 7 kPa was computed as unconfined yield strength (UCS) offset (Δfc) for corn and soybean.

In the case of test materials, cornmeal, corn grits and wheat flour the UCS offset (Δfc) was obtained by measuring the difference between UYS values obtained from both SJSC and ASC at pre-shear consolidation stress of 7 kPa.

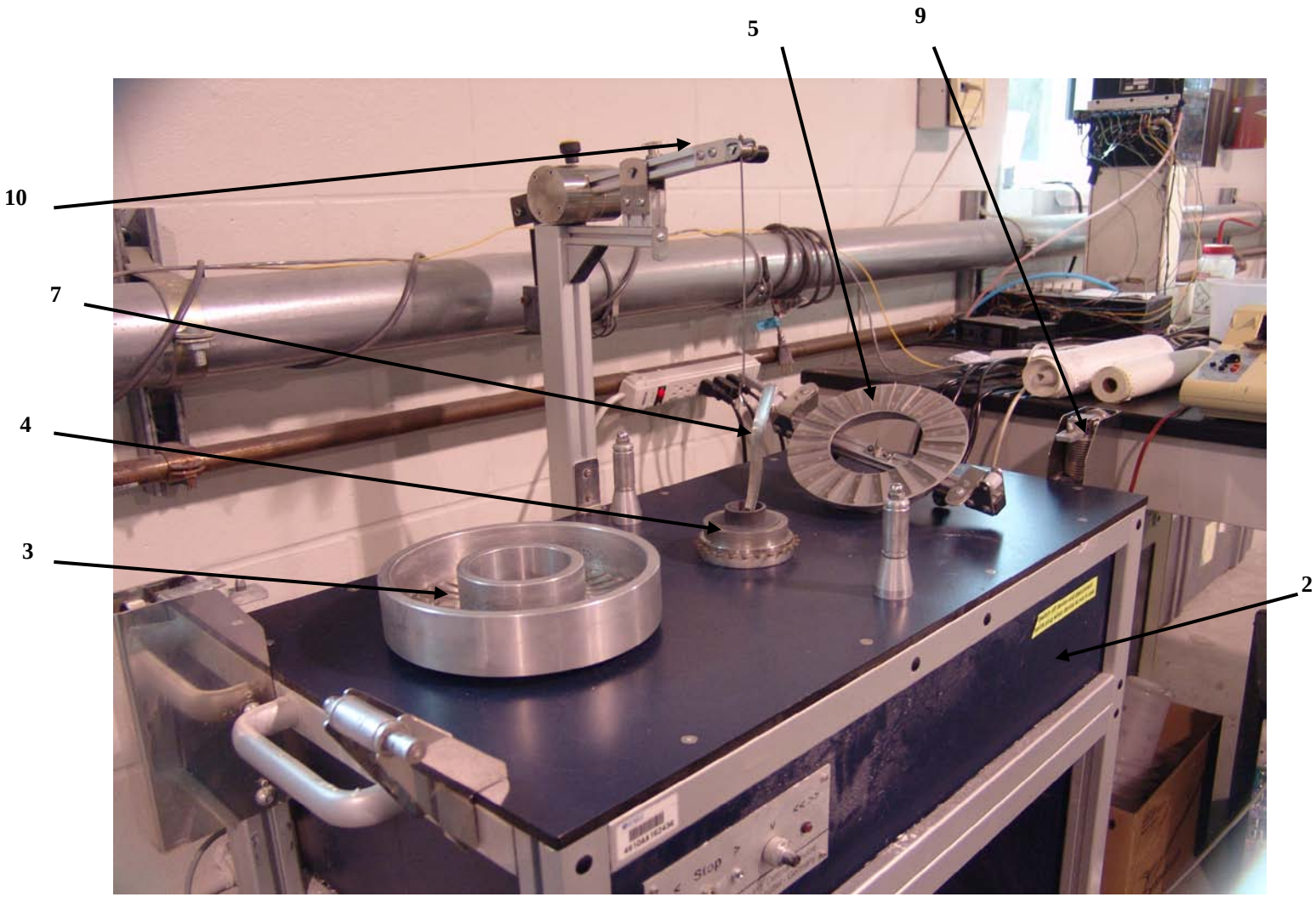

Figure 3-1. The annular shear cell

Figure 3-2. Set-up of the annular shear cell for shear testing

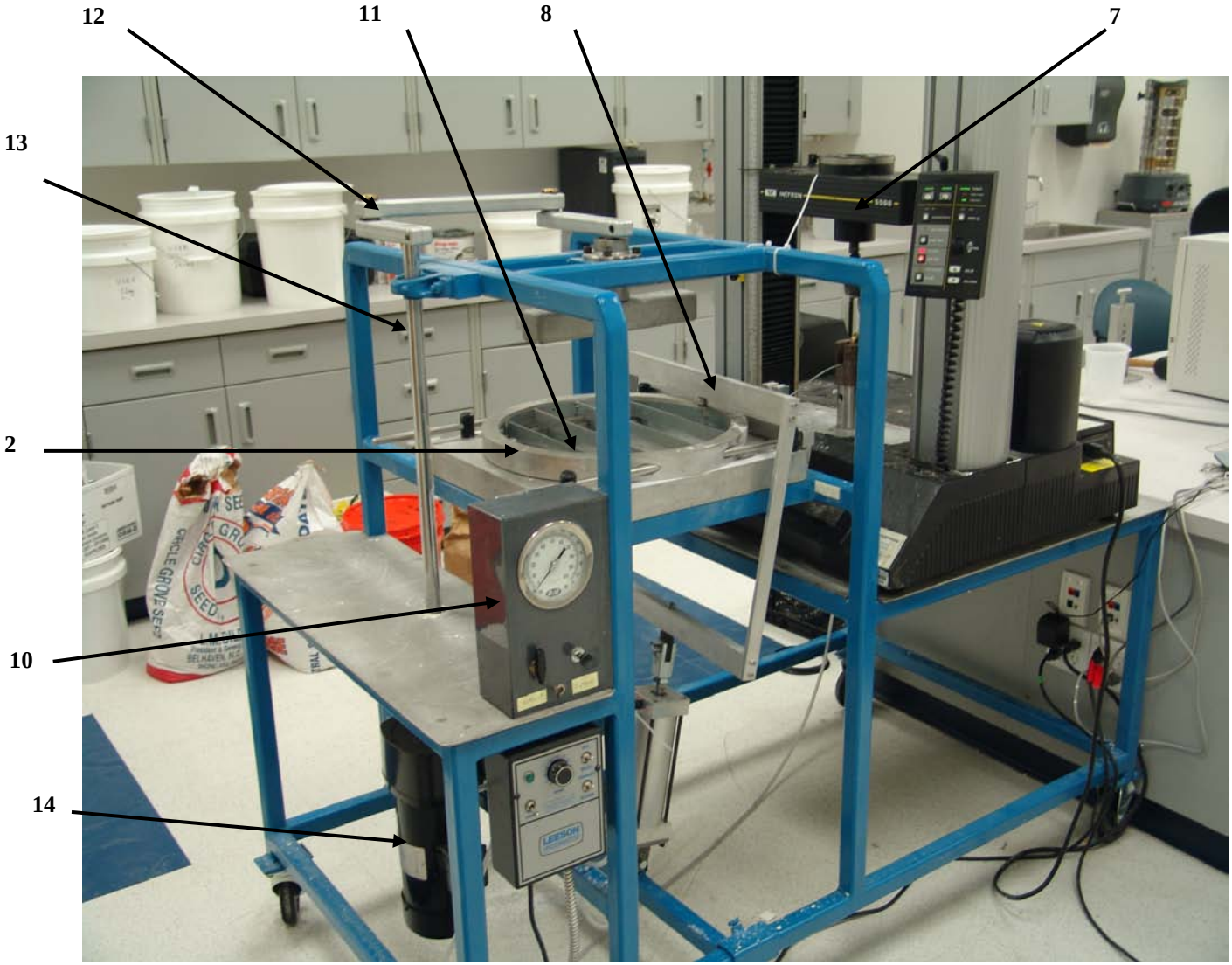

Figure 3-3. The scaled-up Jenike shear cell

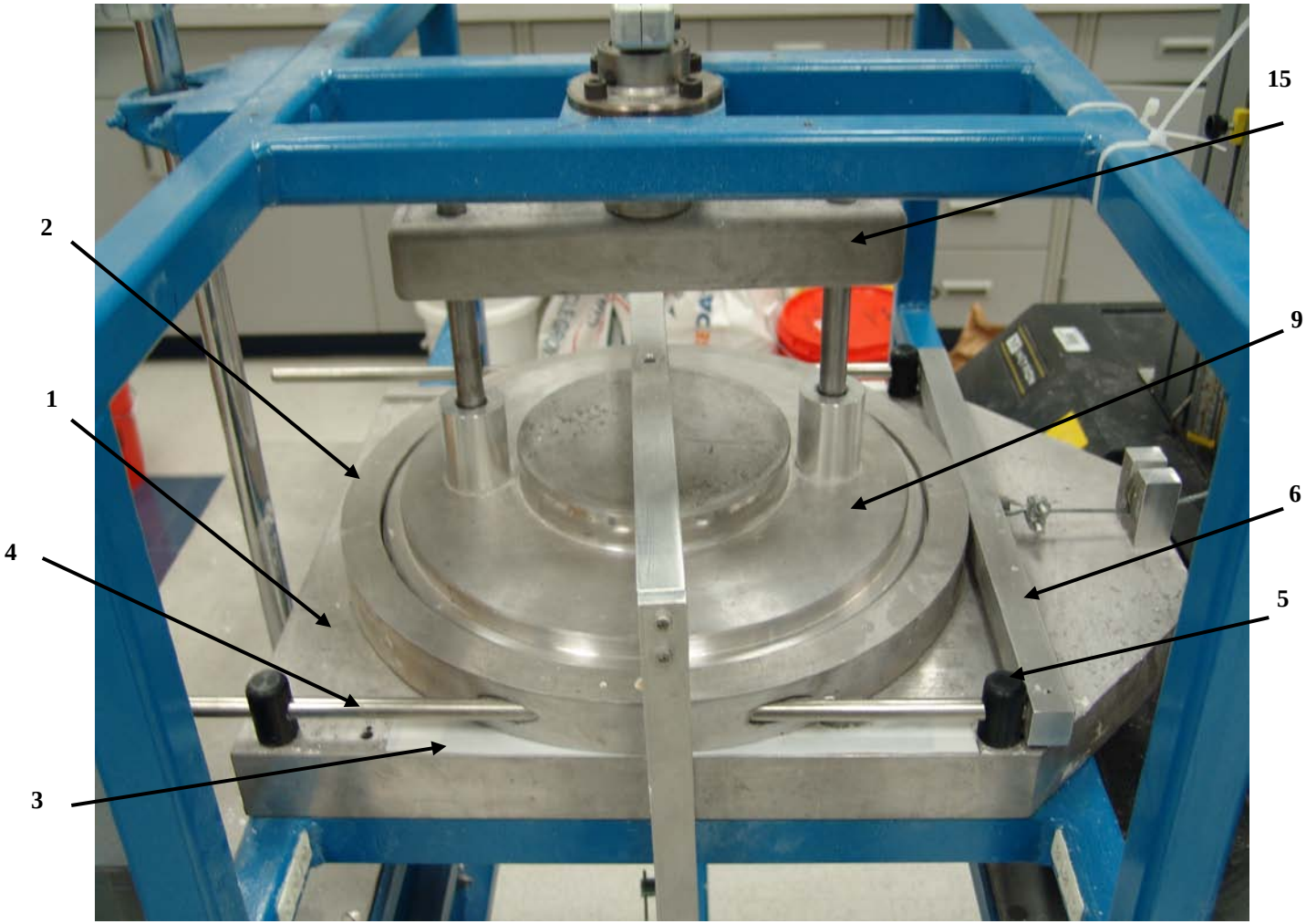

Figure 3-4. SJSC set-up for preconsolidation step

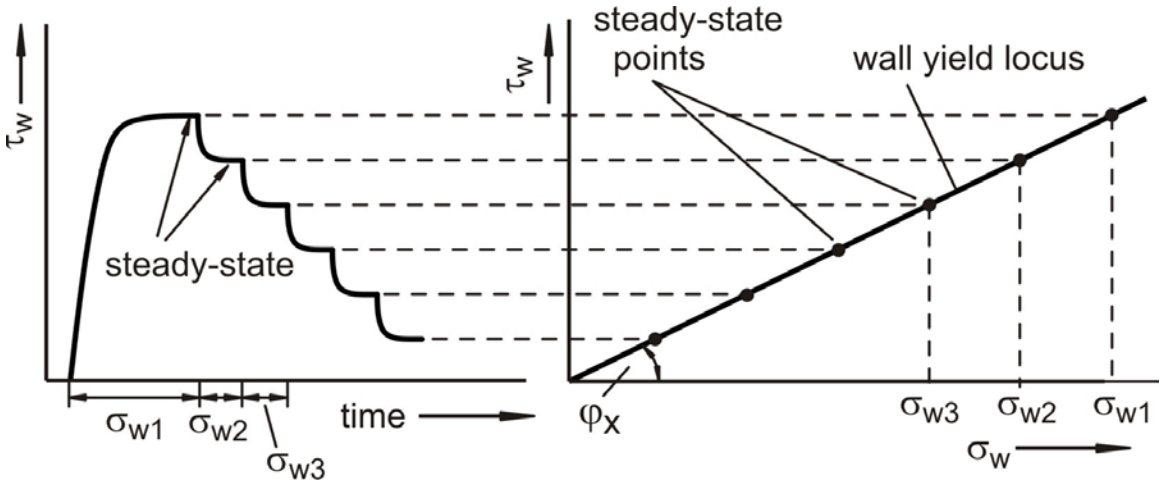

Figure 3-5. Wall friction test: Shear stress versus time and wall yield locus

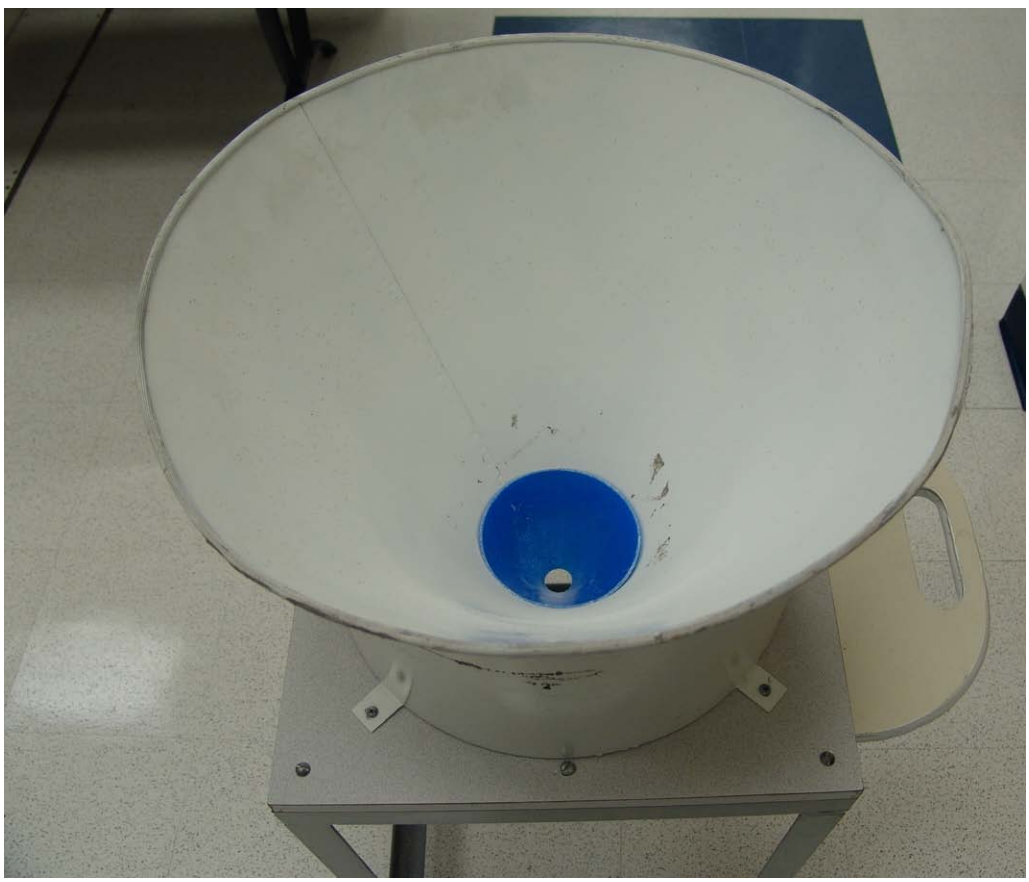

Figure 3-6. Hopper with adjustable outlet size

CHAPTER 4
RESULTS AND DISCUSSION

Shear tests were performed to create four yield loci with five shear points for each test material within normal consolidation stress range of 6 – 13 kPa using both Scaled-up Jenike Shear Cell (SJSC) and Annular Shear Cell (ASC). Test materials corn and soybeans, however, were only tested on the SJSC owing to their relatively large particle size.

Physical Properties

The various physical properties of the six test materials analyzed during the study are summarized in Table 4-1.

Test Data

Figures 4-1 to 4-6 show the typical test data obtained for all the six test materials from SJSC. With the exception of wheat flour, test data from both the testers exhibited a saw-tooth type pattern indicative of slip – stick behavior. The test data obtained from the SJSC showed the shear stress increasing to a maximum and then decreasing until it finally attained a steady value. This indicates that the specimens were probably over – consolidated.

Yield Loci

The yield loci of the six test materials at various normal consolidation stresses using both the shear testers are presented in Figure 4-7 to Figure. 4-14. The yield loci were obtained by linearly regressing the shear stress (τ) versus the normal stress (σ) data and had a correlation coefficient (R^2) between 0.963 – 0.995.

Wall Yield Loci

Wall friction angles for test materials cornmeal, corn grits and wheat flour on an aluminum surface were obtained using a standard Jenike shear cell. Figure 4-15 and Figure 4-16 present the corresponding wall yield loci and wall friction angles respectively. Corn grits had the highest

wall friction angle, although the difference between corn grits and cornmeal was relatively low. Wheat flour as expected had the lowest wall friction angles.

Flow Properties of Test Materials

The flow properties, unconfined yield strength (UYS), angle of internal friction (ϕ) and effective angle of internal friction (δ) of the test materials at corresponding major principle stress (MPS) are listed in table 4-2 to table 4-7. For all cases, (UYS) increased with increase in consolidation stress.

Flow Property Comparison between SJSC and ASC

In order to effectively evaluate the performance of the SJSC, flow properties obtained from SJSC were compared to flow properties from ASC for cornmeal, wheat flour, mung beans and corn grits (Figure 4-17). When compared to ASC, SJSC gave considerably higher unconfined yield strength (UYS) values for cornmeal, mung beans and corn grits; however, SJSC gave substantially lower values for wheat flour. The flow function of test materials corn and soybean obtained from the SJSC was compared to the corresponding flow functions obtained from the hopper test (Figure 4-18). Since only one valid point could be obtained from the hopper the comparison in Figure 4-18 is purely qualitative.

For corn and soybeans, the difference between the flow functions obtained from the SJSC and the hopper test at a pre-shear consolidation stress of 7 kPa were computed as unconfined yield strength (UCS) offset (Δfc). In the case of test materials, cornmeal, corn grits, mung beans and wheat flour, the UCS offset (Δfc) was obtained by measuring the difference between UYS values obtained from both SJSC and ASC at pre-shear consolidation stress of 7 kPa.

The UYS offset (Δfc) of the test materials was plotted as a function of particle size of the test material as shown in Figure 4-19. Corn gave the highest offset, whereas, wheat flour gave a negative offset.

As seen in Figure 4-20, a trend similar to that in UYS values was noticed between angle of internal friction values (ϕ) for cornmeal, mung beans and corn grits. However, ASC gave appreciably higher value for wheat flour.

A comparison between flow properties of SJSC and ASC was completed at a level of significance of 0.05 using the t-test (Kreyszig, 2005). The statistical comparison performed at a level of significance (α) equal to 0.05 showed there were significant differences between the flow properties measured using both the SJSC and ASC for test materials cornmeal, wheat flour, mung beans and corn grits. This was attributed to the high values of UYS, ϕ estimated using SJSC for corn grits and cornmeal and low values for wheat flour.

Probable Factors Influencing Flow Properties Measured From SJSC

From the results discussed, it can be inferred that there is a significant difference between flow properties estimated from SJSC and ASC. Consequently, five influencing factors were identified and are discussed.

Confirm Shear Deformation of Test Material in the SJSC

In order, to qualitatively confirm formation of a shear zone in the SJSC, shear tests were performed with a vertical band of colored particles inserted in the SJSC, across the shear direction. The colored particles helped to visualize the shearing action in the powder bed.

Shear tests were performed with wheat flour and cornmeal. Figure 4-21 and 4-22 illustrate the configuration of the colored particles in the tester at the end of pre-shear for wheat flour and cornmeal respectively. In both cases, the colored particles were displaced along the shear direction. This is possible only if the test material underwent shear deformation in the tester.

Friction at the Base of SJSC

Unlike, the standard Jenike shear cell, the bottom section of the SJSC was not grooved. Grooving is done to increase the surface roughness, thus prevent sliding of the test material at the

base. If the test material, however, slides at the base, the measured unconfined yield strength is in part, a function of friction angle between the material and the base.

Incorporation of sand paper at the base of the SJSC was anticipated as an effective means of increasing roughness (friction). This was confirmed through wall friction test results. Wall friction angles for wheat flour against a smooth flat plate of Aluminum and a rough flat plate with sand paper fastened to its surface were obtained using a standard Jenike shear cell. The effect of surface roughness on wall friction angle is illustrated in Figure. 4-23 and 4-24. In the entire range of investigated wall normal stresses, the wall friction angles for rough sand paper surface were appreciably higher as compared to the smooth aluminum surface.

Consequently, to investigate the effect of increased surface roughness on flow properties of test materials, a circular section of grade 30 sandpaper was adhered to the base of SJSC. A shear test on wheat flour at a pre - shear consolidation stress of 6.9 kPa was performed. Table 4-8 summarizes the comparison between flow properties of wheat flour at a consolidation stress of 6.9 kPa obtained from SJSC with rough sand paper base, SJSC with smooth base and ASC. There was no significant difference between flow properties obtained from SJSC with smooth base and SJSC with rough sand paper base. However, the difference was still significant when compared with the flow properties obtained from the ASC.

Deflection in Steel Rods

Due to the design of SJSC, the steel rods supported on guides can deflect when normal load is applied to the shear lid. The steel rods guide horizontal displacement of the shear ring. A substantial deflection in the rods can obstruct the horizontal displacement of the shear ring, thereby increasing the force required to pull the shear ring along the base. During shear testing, this extra force gets added quantitatively to the measured horizontal force (shear stress), consequently producing discrepancies in the measured data. Shims were placed under the guides

to isolate the shear ring from the base and a normal stress of 12 kPa was applied to the shear ring. The empty ring was then sheared and midway the deflection in the steel rods was measured using a digital micrometer. Since the steel rods had an overhang, the slope was measured using a digital angle gauge.

At 12 kPa, the deflection in the rods was 0.007 mm with a slope of 0.5^0. The measured deflection is moderately low, but the slope can cause elastic deformation between steel rods and Teflon guides. Figure 4-25 illustrates the tangential force required to displace the shear ring loaded under 12 kPa of normal stress. The tangential force rather than being constant, increases with shear distance. This continuous increase can be attributed to the slope of 0.5^0.

However, in an actual shear test performed under a maximum normal consolidation stress of 12 kPa, the shear ring rests on the base and the material not the shear ring is subjected to load. Hence, due to friction only a fraction of normal force gets transferred to the steel rods and any associated deflection can be neglected.

Friction between Steel Rods and Guides

Since the steel rods slide through the guides, it is worth considering the friction force arising at the rod-guide contact. Since the shear ring rested on the Teflon strips attached to the base, friction between the shear ring and the base was also accounted for in this analysis.

To evaluate the magnitude of normal force to be applied to the shear ring, a force balance (Figure 4-26) was set up on the shear ring having a cross section area A, curved surface area u and height h. A constant vertical stress σ_v is acting across the cross-section. Assuming Janssen's k = 0.5, a lateral stress σ_h is acting in the horizontal direction. Due to wall and material friction occurring in the ring, friction force (F) is set up in the ring.

$$k = \frac{\sigma_h}{\sigma_v} \tag{4-1}$$

where σ_h: lateral stress (kPa)
σ_v: vertical stress (kPa)

$$\tan\phi_x = \frac{F}{\sigma_h uh} \tag{4-2}$$

where ϕ_x: wall friction angle (degrees)
F: friction force (N)
u: circumference of the ring (m)
h: height of the ring (m)

Assuming shear ring is filled with corn grits and 12 kPa of normal stress is applied, solving Equations 4-1 and Equation4-2 gives F = 106.01 N. Subsequently, normal force (F) was applied to the empty shear ring, and the tangential force (H) required to displace the ring was measured.

The tangential force (H) was a measure of excess force spent while shearing a material, the friction force (H) could be subtracted from the net shear force required to pre - shear the material. Similar analyses were repeated for different consolidation stresses and corresponding failure stresses and the flow properties of all the test materials were recalculated. A comparison between the original UYS offset and reduced UYS offset after normalizing the data for friction is shown in Figure 4-27.

Normal stress Inhomogeneity in SJSC

Bilgili, et al. (2004) discussed the spatiotemporal variation of the normal stress in a standard Jenike shear cell. They found that during pre-shear, a skewed normal stress profile develops with the highest stress towards the leading edge of the cell. This tendency can lead to local bulk density variation in the test material present in the shear cell.

Penetration tests were performed on wheat flour to observe local bulk density variations along the shearing direction in the SJSC. A hollow cylindrical sampler 63.5 mm in diameter and 101.6 mm. long was used to retrieve samples of wheat flour (pre-sheared at 8 kPa) from the tester's powder bed. The sharp end of the sampler easily penetrated the flour bed and was gently

pushed down until it reached the tester bottom. Care was taken to not disturb the local stress state. Upon, reaching the bottom, the sampler was carefully ejected out of the powder bed, thus, retrieving a cylindrical plug of wheat flour.

As shown in Figure 4-28, the wheat flour sample still housed in the sampler was placed under the crossbar of the Instron. The Instron was set up such that the flour surface could be loaded with a force of 6 N in 2 seconds (Figure. 4-28). A frustum-shaped cross-head was attached to Instron's load cell and the penetration height due to loading was recorded. Penetration tests were performed on samples retrieved at a distance of 19, 235, 295 mm form the shearing edge. Figure 4-29 shows typical penetration test data. Figure 4-30 illustrates the increase in penetration heights in three samples retrieved from the tester's powder bed.

Penetration height is an inverse function of bulk density of the material. The relative increase in penetration heights across the length of the SJSC indicates that the bulk density of wheat flour decreases from the shearing edge to the leading edge. Since bulk density is a function of normal stress acting on the material, the bulk density variation indicates that during shearing, normal stress variation occurs in the SJSC. Due to the normal stress variation, wheat flour undergoes partial shearing and partial consolidation. As a result, lower shear stress values for pre-shear and shear points were obtained from the shear tests. Consequently, the yield locus generated from these points yielded significantly lower values of unconfined yield strength for wheat flour.

Offset Analysis

A least square analysis was performed on cohesion (c) and angle of internal friction (ϕ) values obtained from the SJSC's yield loci. The objective was to determine the offset necessary in c and ϕ, such that the flow function obtained from the SJSC would be identical to that obtained from the ASC for test materials cornmeal, mung beans and corn grits.

A solving block was set up in a spreadsheet application (Microsoft Excel) to minimize the square of the error in the flow functions represented by the following error function

$$E = \left(1 - \frac{b_S}{b_A}\right)^2 + \left(1 - \frac{m_S}{m_A}\right)^2 \tag{4-3}$$

where b_S: y-intercept of flow function from SJSC (Pa)
b_A: y-intercept of flow function from ASC (Pa)
m_S: slope of flow function from SJSC
m_A: slope of flow function from ASC

The results for cornmeal (Figure 4-31) indicated that an offset of -137.54 Pa and 0.08^o was required in c and ϕ values. A similar analysis performed on corn grits and mung beans and the offset values are listed in table 4-9.

Since the offset values for cornmeal, mung beans and corn grits were different, the offset was a function of the bulk specimen. This functionality was expressed in terms of particle size of the test materials.

Since shear tests on corn and soybean could only be performed on the SJSC, so offset analysis could not be performed for these test materials. As a result, due to lack of experimental data, correction factors were estimated. A linear relationship was assumed to exist between the particle size and the corresponding offset values (c and ϕ) for cornmeal, and corn grits. This relationship was extrapolated to particle size corresponding to corn and soybeans and then correction factors were predicted. For corn, the correction factors for c and ϕ were -1017.05 Pa and 17.77^o respectively and for soybeans the correction factor for c and ϕ were -772.48 Pa and 12.85^o respectively. Upon applying the correction factor to the flow property data for corn and soybeans negative values for unconfined yield strength were obtained (Figure 4-32). This was incorrect, since the values obtained from the hopper test indicate at least one positive value for UYS for both corn and soybeans.

Subsequently, c and ϕ offset values for mung beans were included in the linear relationships that were used to predict correction factors for corn and soybeans. The linear relationship for c versus particle size had a correlation coefficient (R^2) value of 0.861 and the linear relationship between ϕ and particle size had a correlation coefficient (R^2) value of 0.458, which was quite low. These relationships were extrapolated to particle size corresponding to corn and soybeans and the correction factors were again estimated. For corn, the correction factors for c and ϕ were -474.19 Pa and 2.72^o respectively and for soybeans the correction factor for c and ϕ were -367.54 Pa and 2.12^o respectively. These correction factors were applied to the flow property data for soybeans and corn and the resulting flow function are shown in Figure 4-32 and Figure 4-33 respectively. Application of the correction factor to the flow property data for corn and soybeans produced good agreement between the strength values obtained from the hopper tests and the corrected strength values. Since the correlation coefficient value for the linear relationship between ϕ and particle size was very low, it introduced uncertainty in the estimated ϕ correction factors. Also, a power law relationship could not be used with entire certainty, because incorporation of additional data points could have increased the correlation coefficient's value, whereby a linear relationship could have been established. As a result, still better estimates for the relationship between the offset values and particle size are required and can be obtained by including more points in the offset analysis. This could be realized by testing a still wider range of bulk solids on both the ASC and SJSC.

Table 4-1. Physical properties of the test materials

Test material	Moisture content (%wb)	Bulk density (kg m^{-3})	Mean particle diameter (mm)
Wheat flour	12.2	710	0.049
Cornmeal	13.4	680	0.8
Corn grits	9.4	740	1.3
Mung beans	5.6	880	3.9
Soybeans	6.3	740	6.6
Corn	6.2	780	8.2

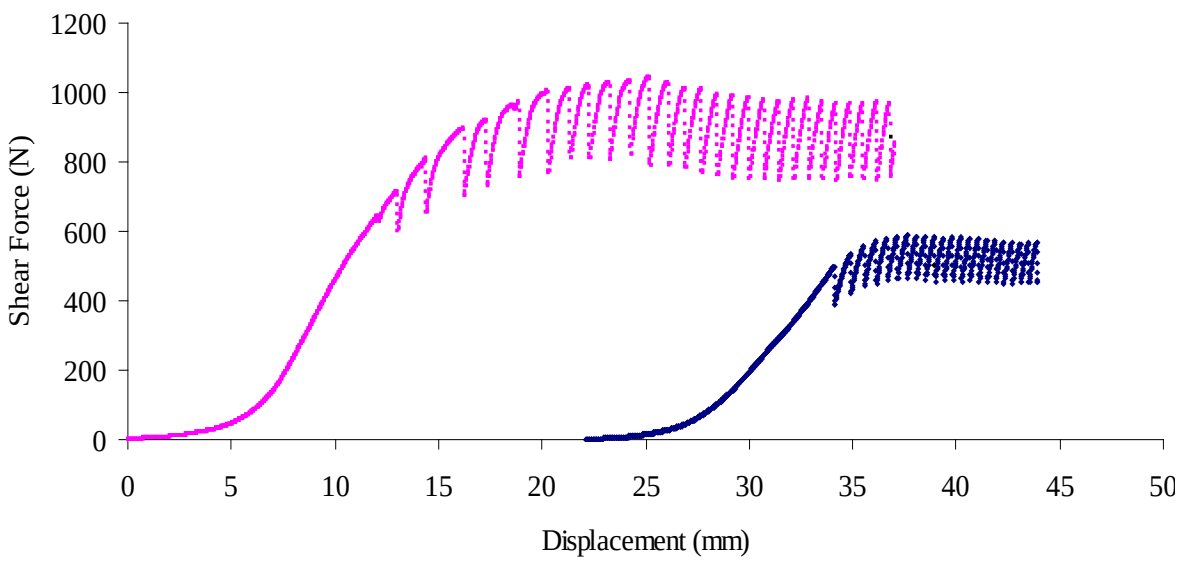

Figure 4-1. Typical SJSC test data for cornmeal

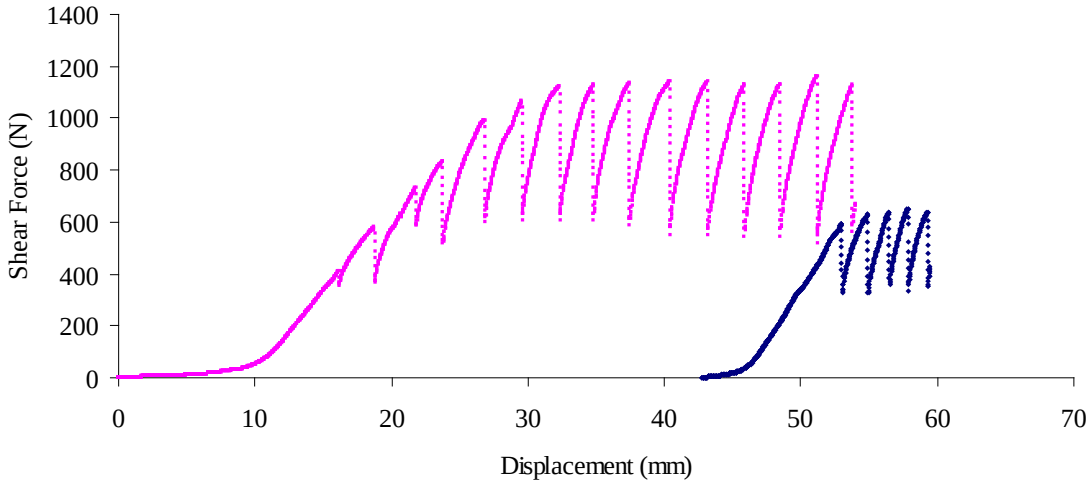

Figure 4-2. Typical SJSC test data for corn grits

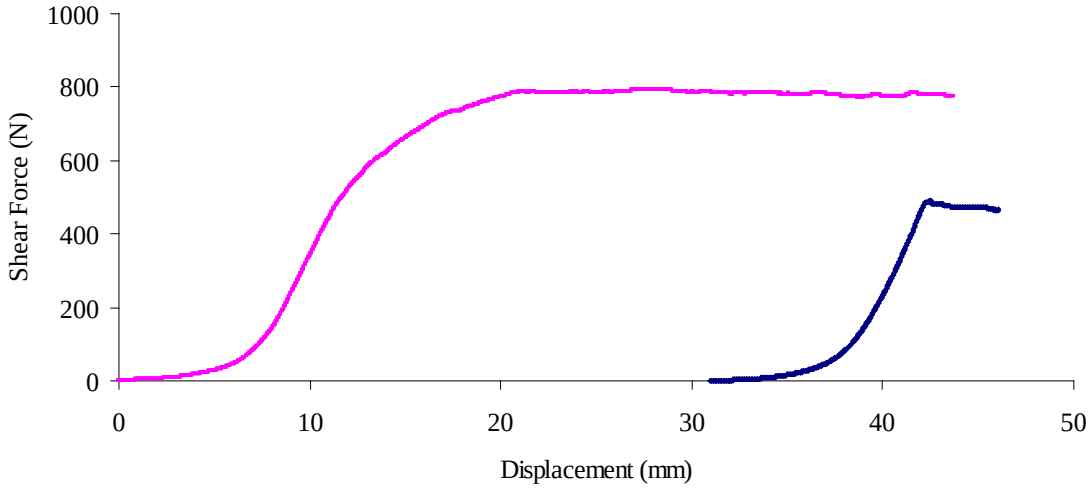

Figure 4-3. Typical SJSC test data for wheat flour

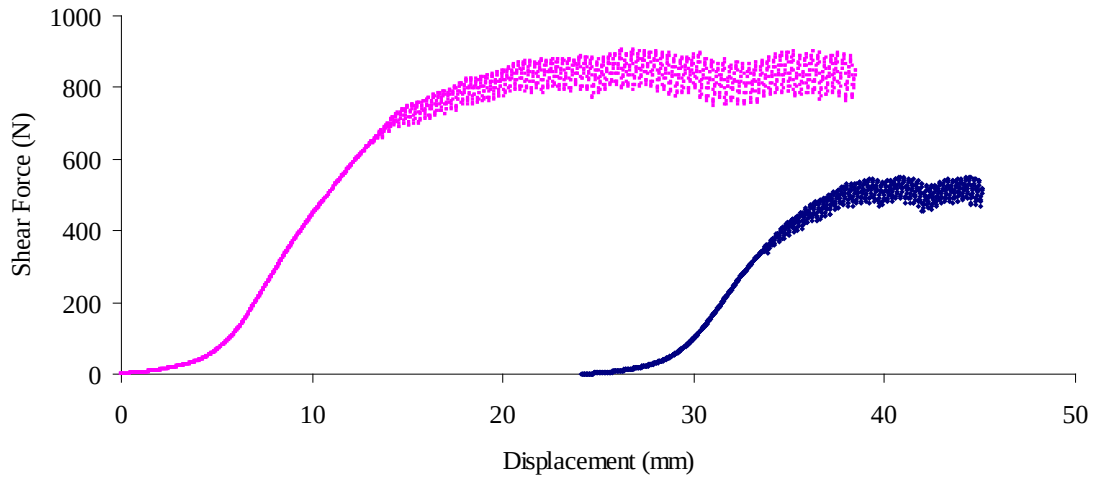

Figure 4-4. Typical SJSC test data for corn

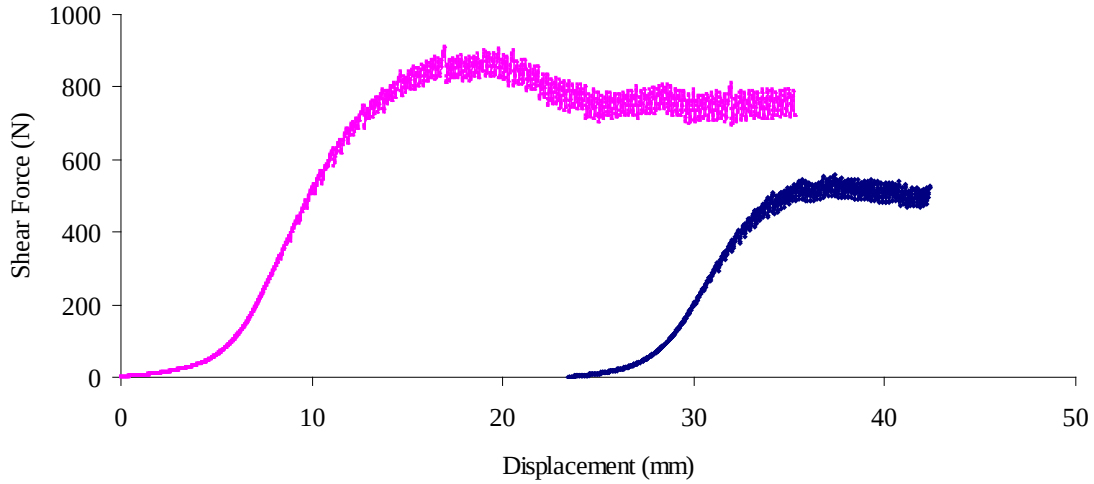

Figure 4-5. Typical SJSC test data for soybeans

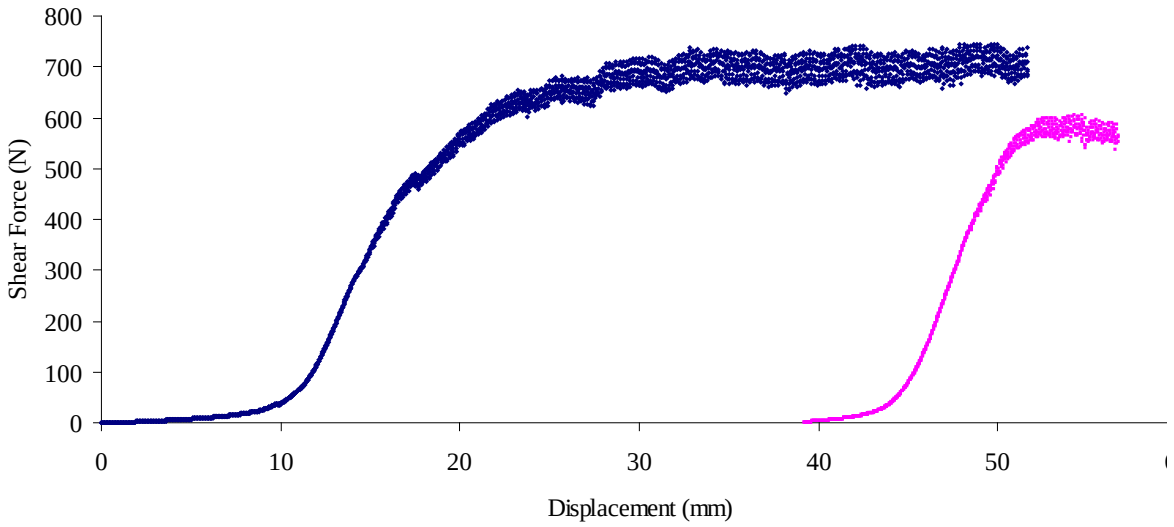

Figure 4-6. Typical SJSC test data for mung beans

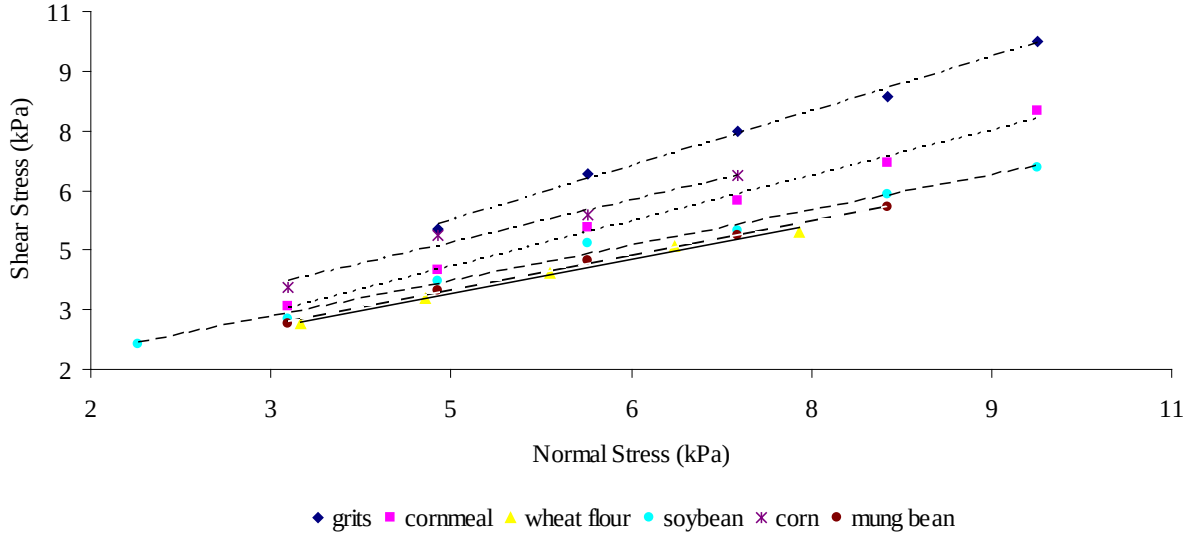

Figure 4-7. SJSC yield loci at normal consolidation stress 13.1 kPa

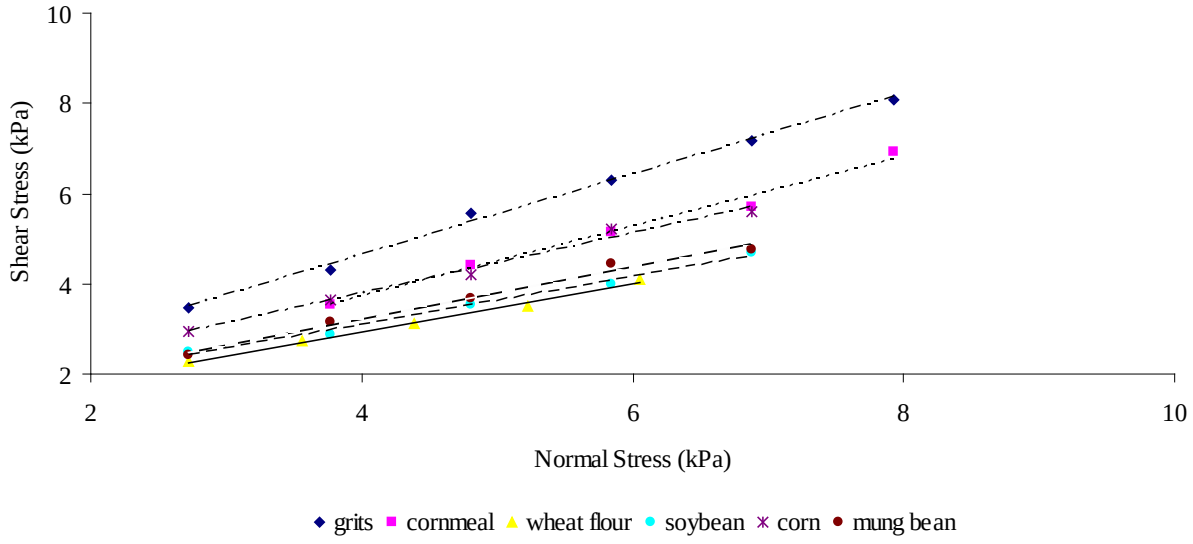

Figure 4-8. SJSC yield loci at normal consolidation stress 11.03 kPa

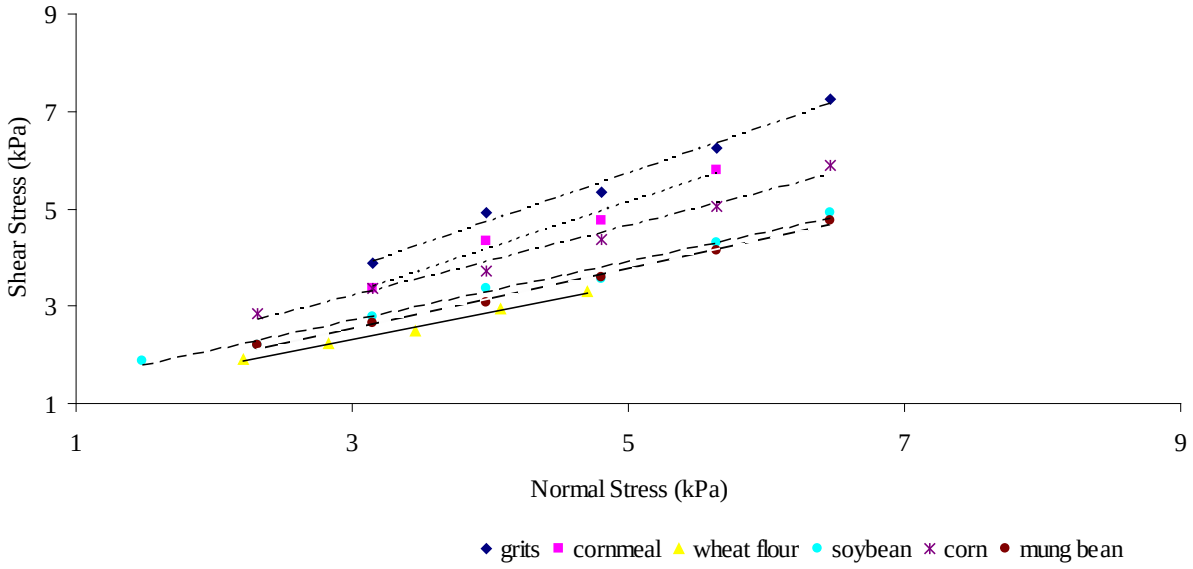

Figure 4-9. SJSC yield loci at normal consolidation stress 8.9 kPa

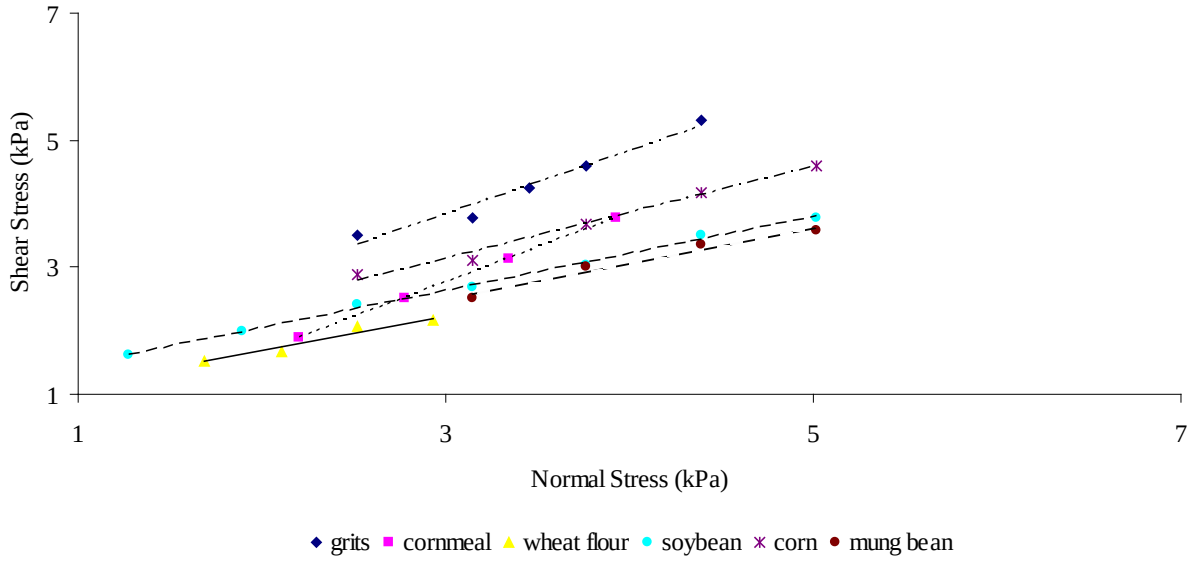

Figure 4-10. SJSC yield loci at normal consolidation stress 6.9 kPa

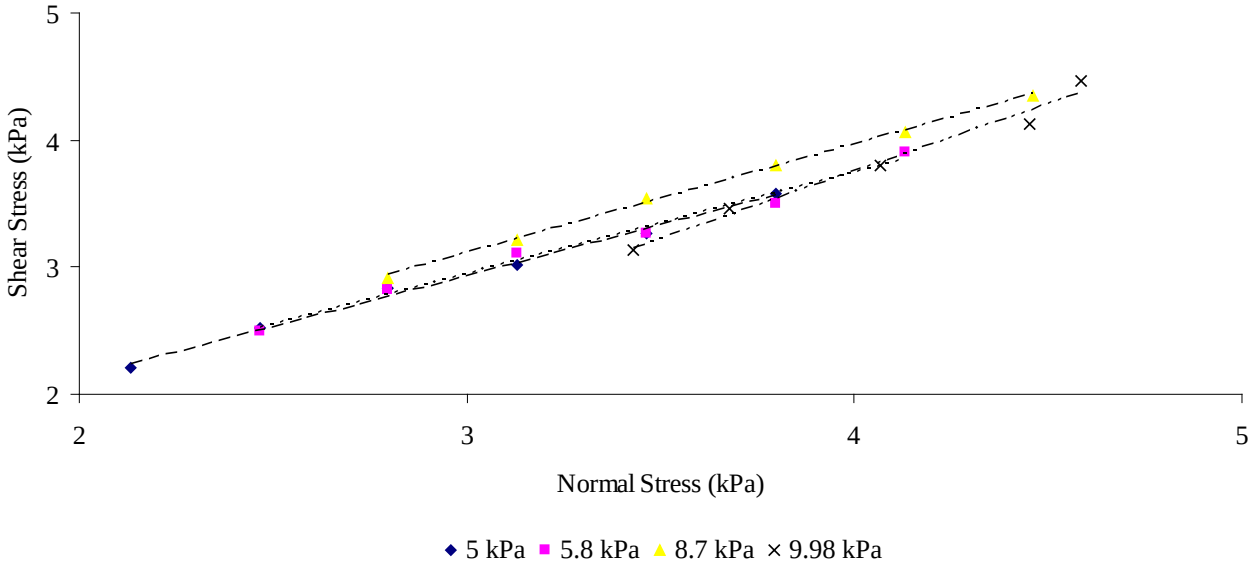

Figure 4-11. ASC yield loci for corn grits

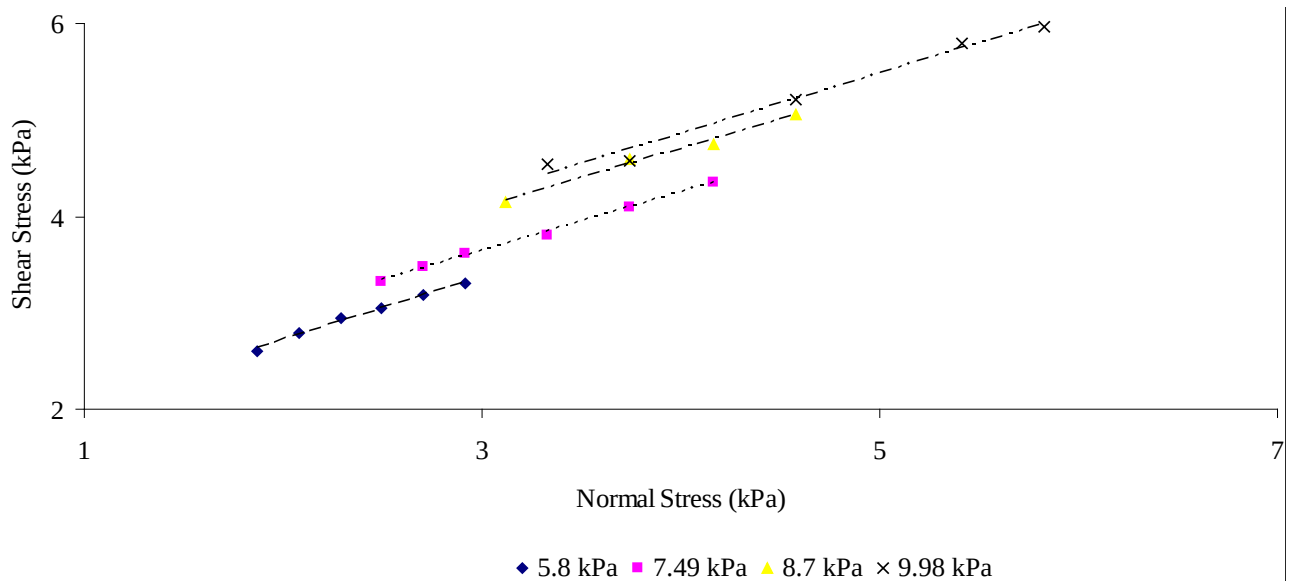

Figure 4-12. ASC yield loci for wheat flour

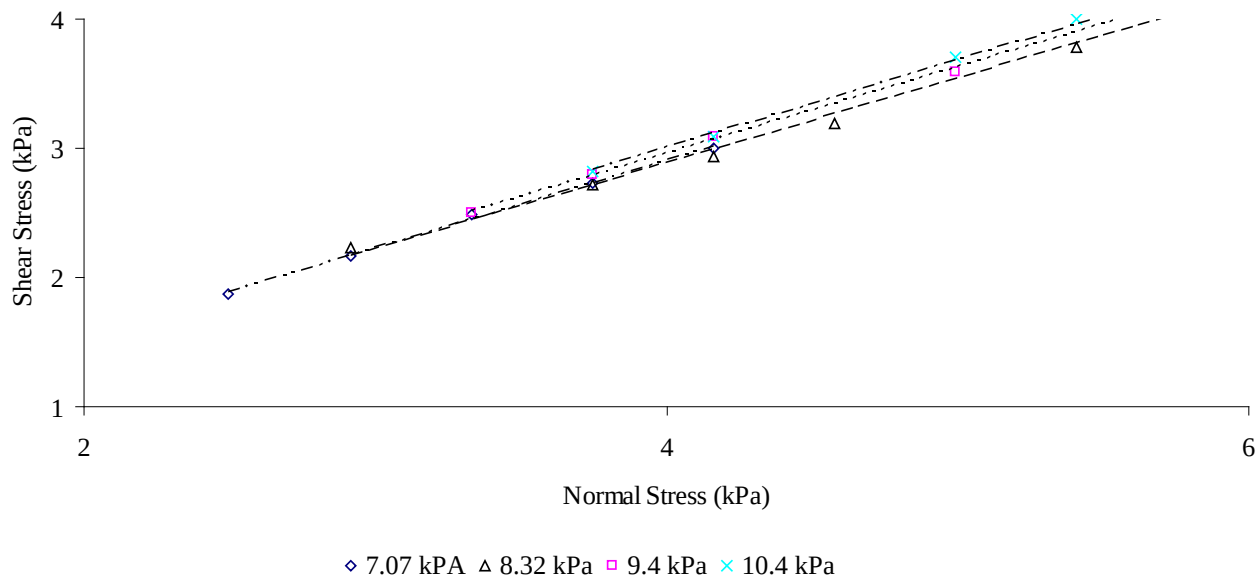

Figure 4-13. ASC yield loci for cornmeal

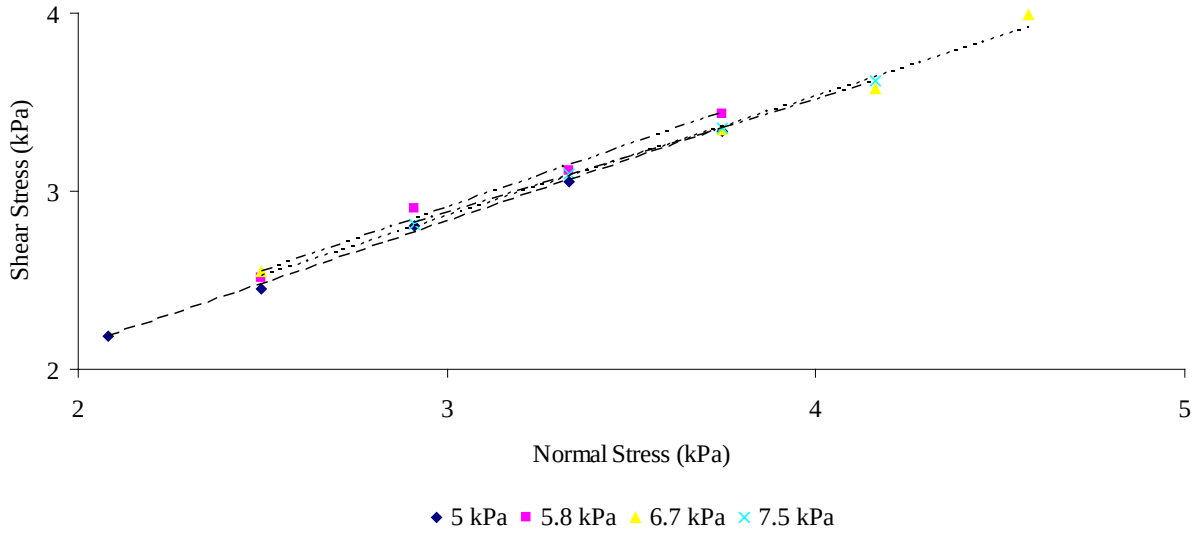

Figure 4-14. ASC yield loci for mung beans

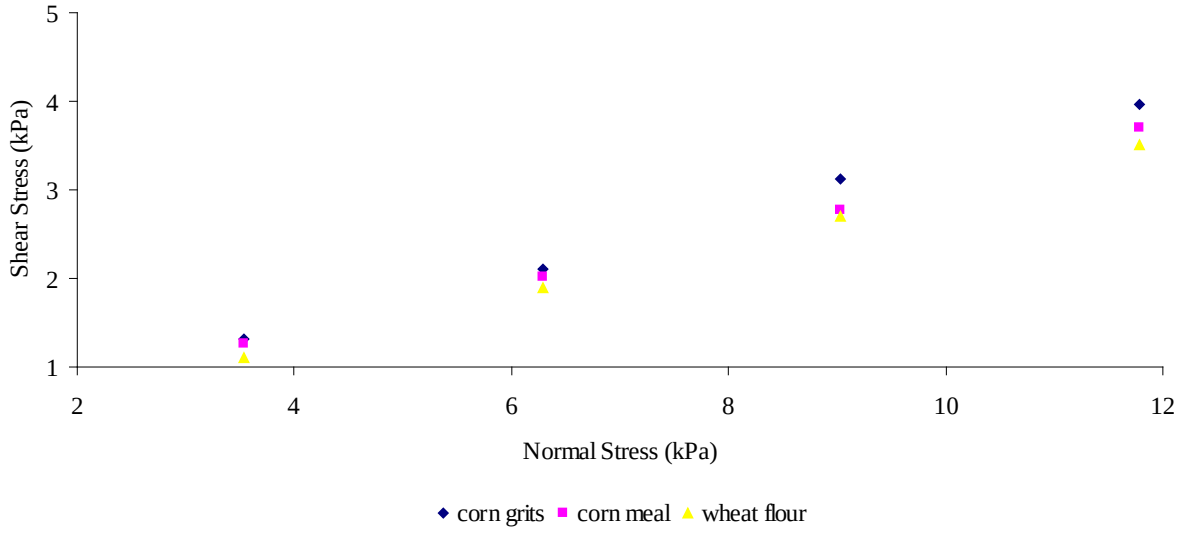

Figure 4-15. Wall yield loci for corn grits, cornmeal, wheat flour

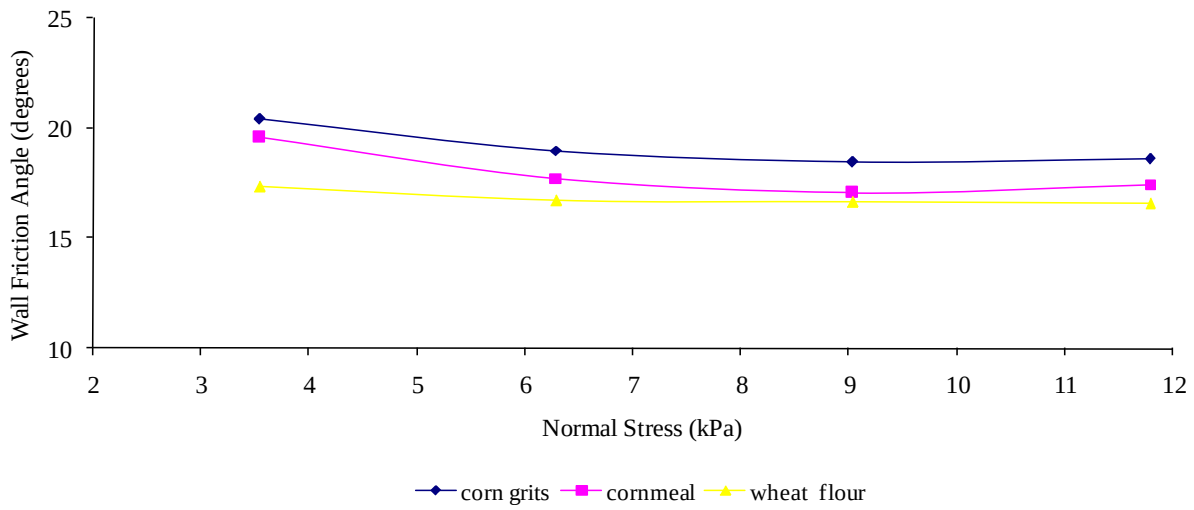

Figure 4-16. Wall friction angles for corn grits, cornmeal wheat flour

Table 4-2. Flow properties measured by SJSC and ASC for cornmeal

Test method	Consolidation stress (kPa)	MPS (kPa)	UYS (kPa)	Angle of internal friction (degrees)	Effective angle of internal friction (degrees)
SJSC	6.9	14.2	1.36	42.7	44.8
	8.9	19.7	1.63	42.8	44.6
	11.0	24.9	2.06	37.5	39.5
	13.1	30.9	2.11	37.1	38.7
ASC	7.1	14.7	0.75	34.0	35.3
	8.3	17.3	0.95	33.3	34.6
	9.4	19.9	1.05	33.8	35.1
	10.4	22.1	1.11	34.1	35.4

Table 4-3. Flow properties measured by SJSC and ASC for corn grits

Test method	Consolidation stress (kPa)	MPS (kPa)	UYS (kPa)	Angle of internal friction (degrees)	Effective angle of internal friction (degrees)
SJSC	6.9	17.7	3.27	44.9	48.9
	8.9	25.3	3.44	43.9	46.9
	11.0	32.9	4.14	41.5	44.3
	13.1	37.5	4.43	42.2	44.8
ASC	5.0	12.7	1.98	38.5	42.2
	5.8	15.9	2.02	38.6	41.6
	7.1	18.6	2.36	40.4	43.3
	8.3	21.9	2.64	42.9	45.5

Table 4-4. Flow properties measured by SJSC and ASC for wheat flour

Test method	Consolidation stress (kPa)	MPS (kPa)	UYS (kPa)	Angle of internal friction (degrees)	Effective angle of internal friction (degrees)
SJSC	4.8	6.9	2.01	28.6	36.9
	6.9	10.5	2.24	29.0	34.9
	8.9	13.7	2.70	27.9	33.4
	11.0	17.3	2.86	29.7	34.1
ASC					
	5.8	9.4	5.19	33.5	50.5
	7.5	11.9	6.46	31.3	48.3
	8.7	13.8	8.10	31.1	53.0
	9.9	15.7	8.54	31.9	48.9

Table 4-5. Flow properties measured by SJSC for corn

Test method	Consolidation stress (kPa)	MPS (kPa)	UYS (kPa)	Angle of internal friction (degrees)	Effective angle of internal friction (degrees)
SJSC	6.9	15.1	3.21	35.8	41.2
	8.9	18.7	3.55	35.6	40.4
	11.0	20.9	3.64	33.6	38.0
	13.1	25.6	5.11	35.6	40.6

Table 4-6. Flow properties measured by SJSC and ASC for soybeans

Test method	Consolidation stress (kPa)	MPS (kPa)	UYS (kPa)	Angle of internal friction (degrees)	Effective angle of internal friction (degrees)
SJSC	6.9	14.8	2.37	31.2	35.3
	8.9	17.4	2.53	31.4	35.2
	11.0	20.8	2.76	27.9	31.4
	13.1	24.4	3.13	30.7	34.1

Table 4-7. Flow properties measured by SJSC and ASC for mung beans

Test method	Consolidation stress (kPa)	MCS (kPa)	UYS (kPa)	Angle of internal friction (degrees)	Effective angle of internal friction (degrees)
SJSC	6.9	13.4	2.31	31.9	36.4
	8.9	16.6	2.52	31.6	35.5
	11.0	20.1	3.16	30.1	34.2
	13.1	22.8	3.31	30.2	33.7
ASC					
	5.0	9.2	0.87	35.0	37.3
	5.8	11.0	1.00	35.6	37.8
	6.7	13.1	1.29	33.9	36.4
	7.5	14.4	1.68	32.6	35.5

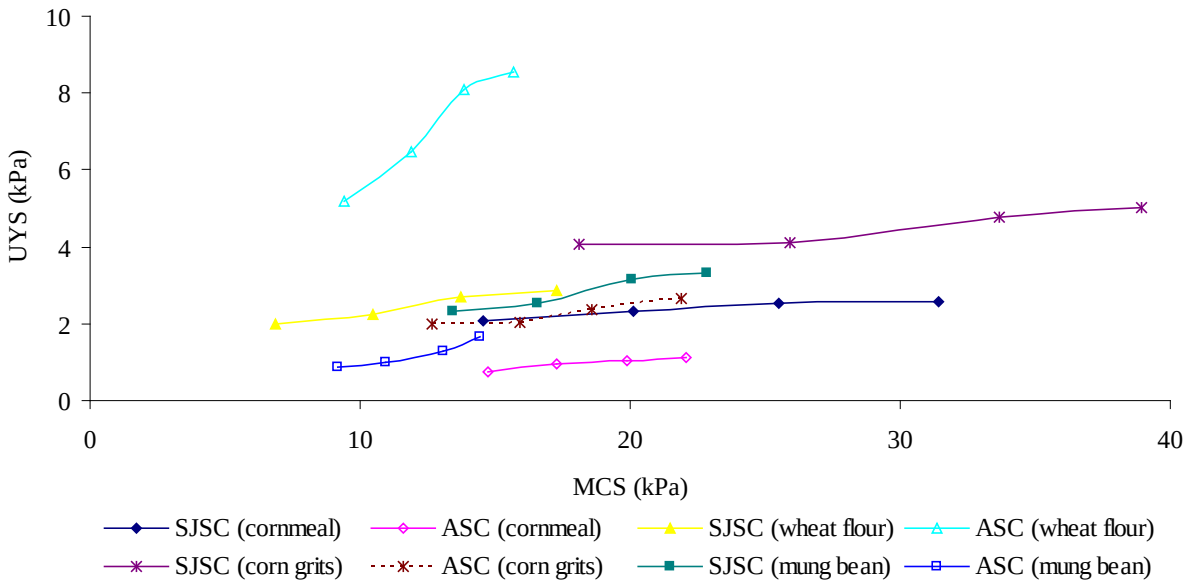

Figure 4-17. Comparison of flow functions of test materials from SJSC and ASC

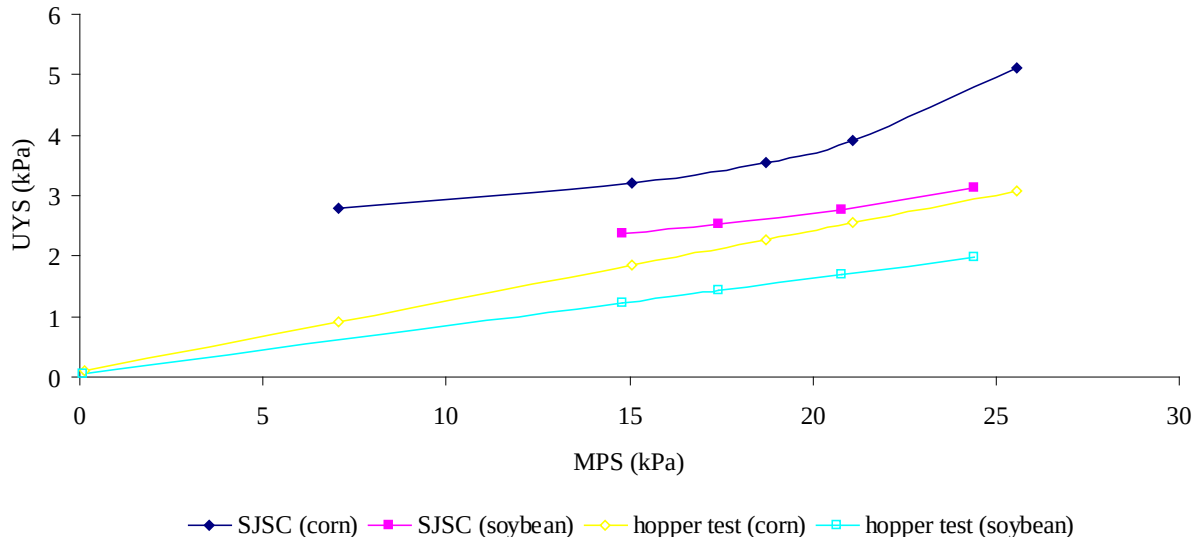

Figure 4-18. Comparison of flow function of corn and soybeans from SJSC and hopper test

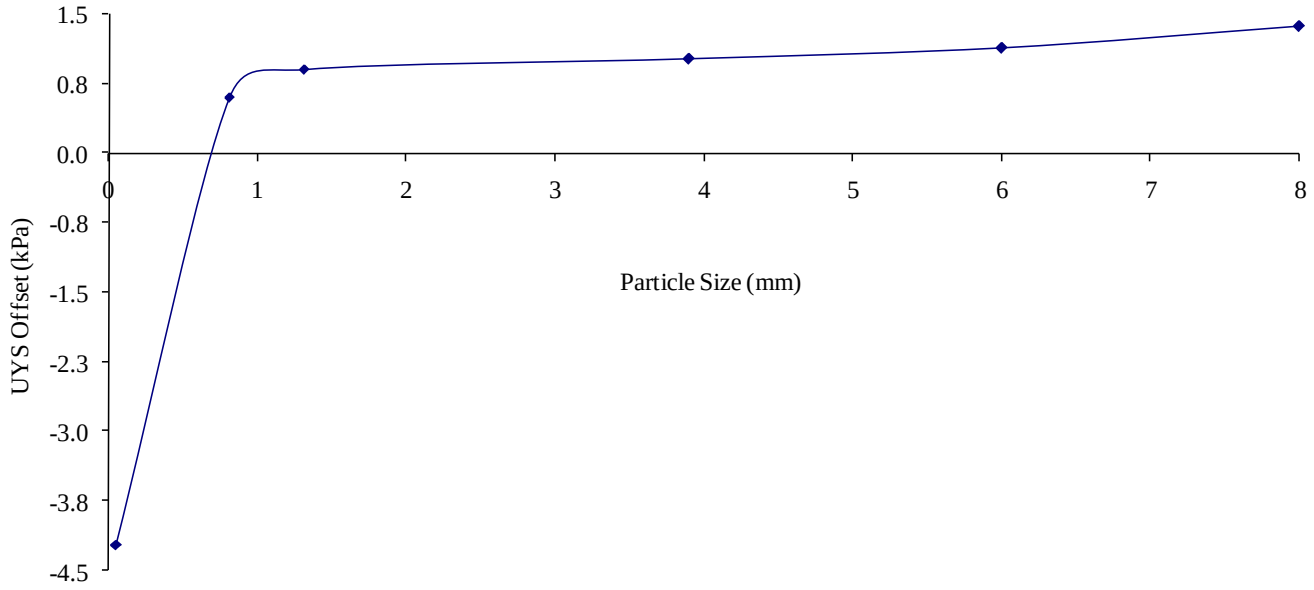

Figure 4-19. Offset in unconfined yield strength at consolidation stress of 7 kPa

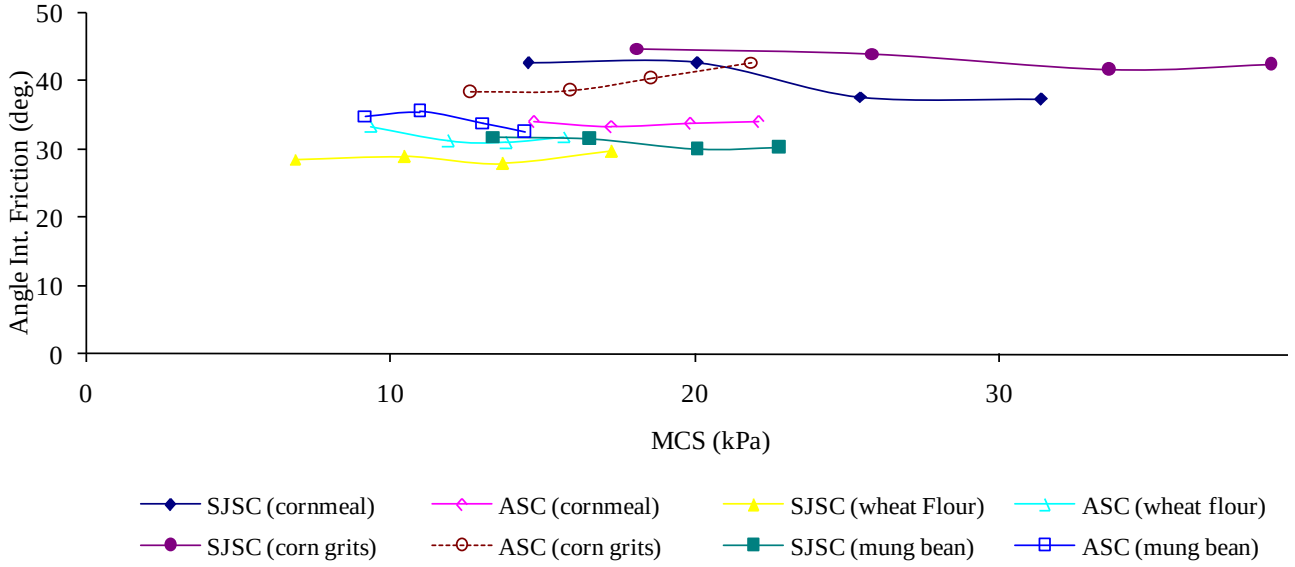

Figure 4-20. Comparison of angle of internal friction of test materials from SJSC and ASC

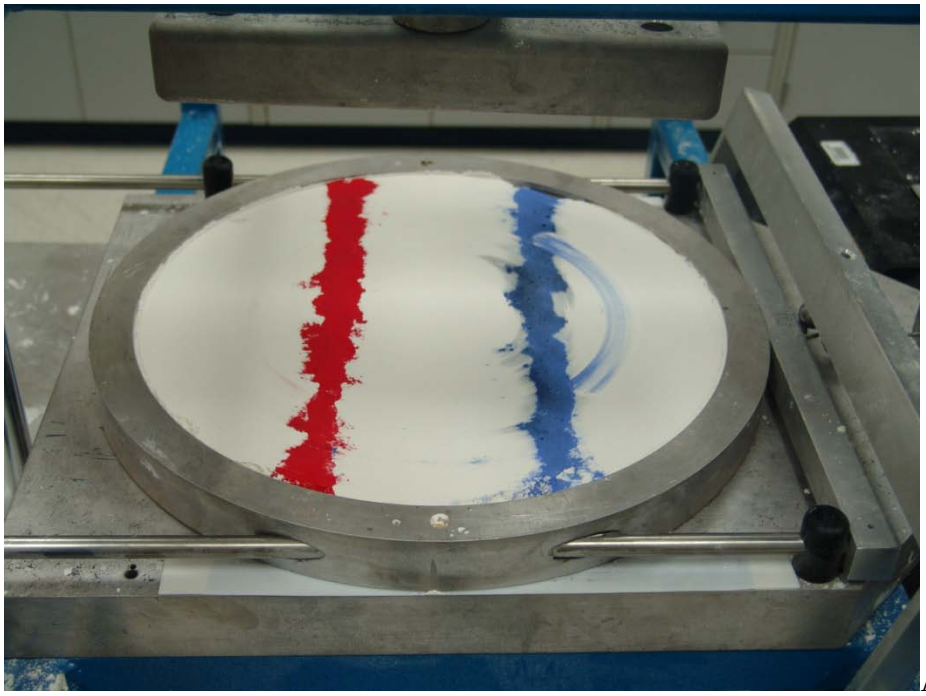

A

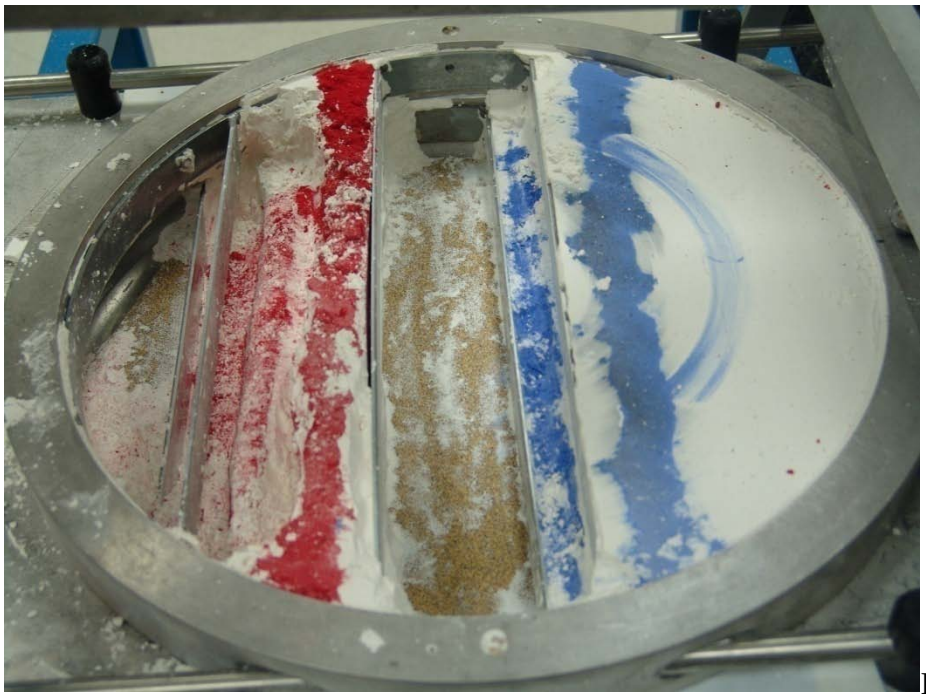

B

Figure 4-21. Shear deformation test on wheat flour. A) Prepared specimen before pre-shear, B) Shear deformation occurring towards the right as indicated by the red color.

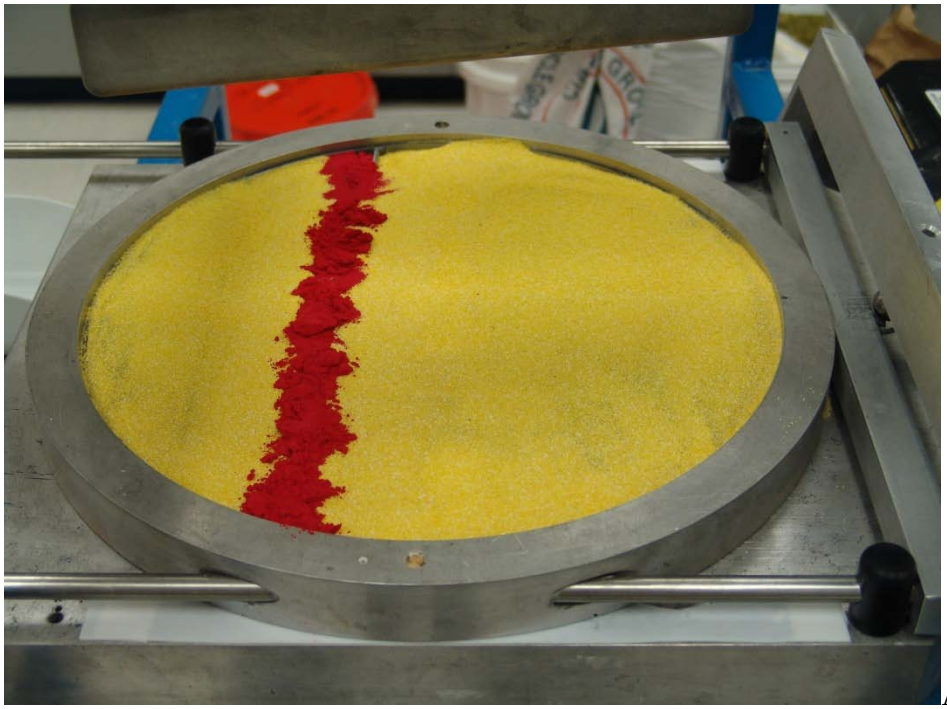
A

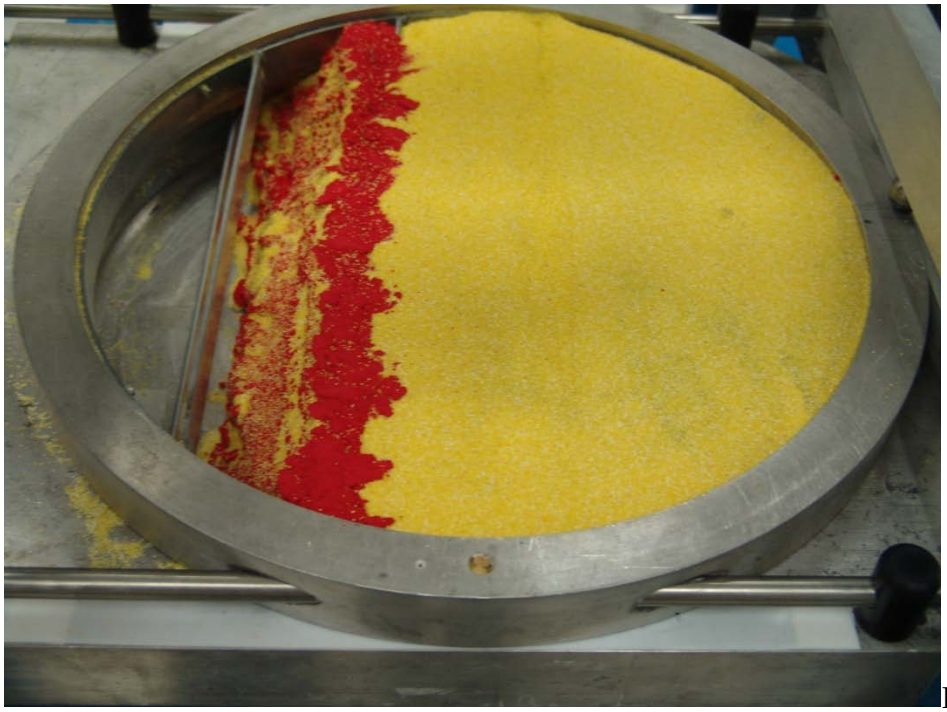
B

Figure 4-22. Shear deformation test on corn meal. A) Prepared specimen before pre-shear, B) Shear deformation occurring towards the right as indicated by the red color

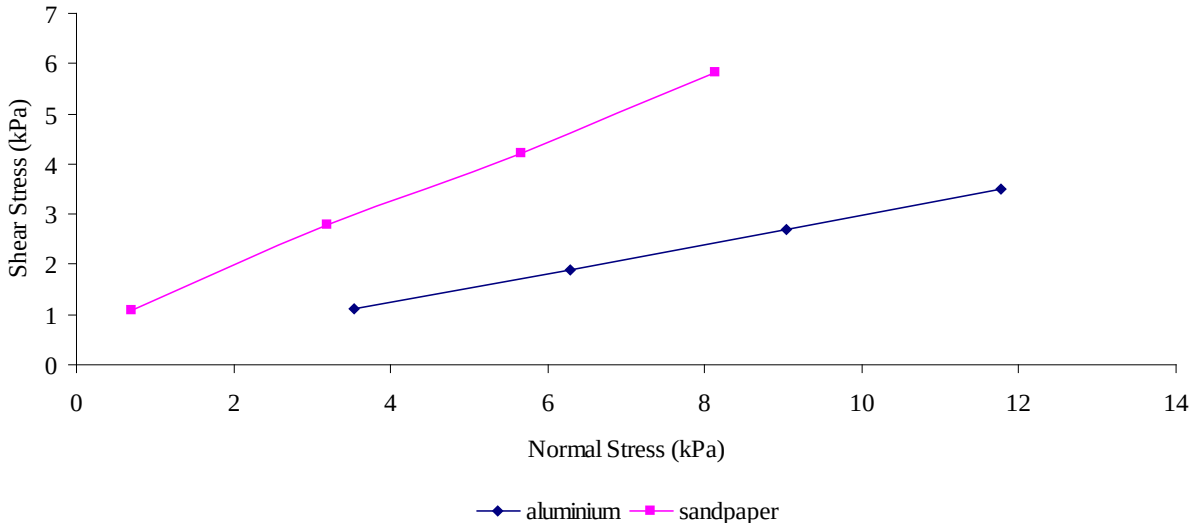

Figure 4-23. Wall yield loci for wheat flour on aluminum and sandpaper surface

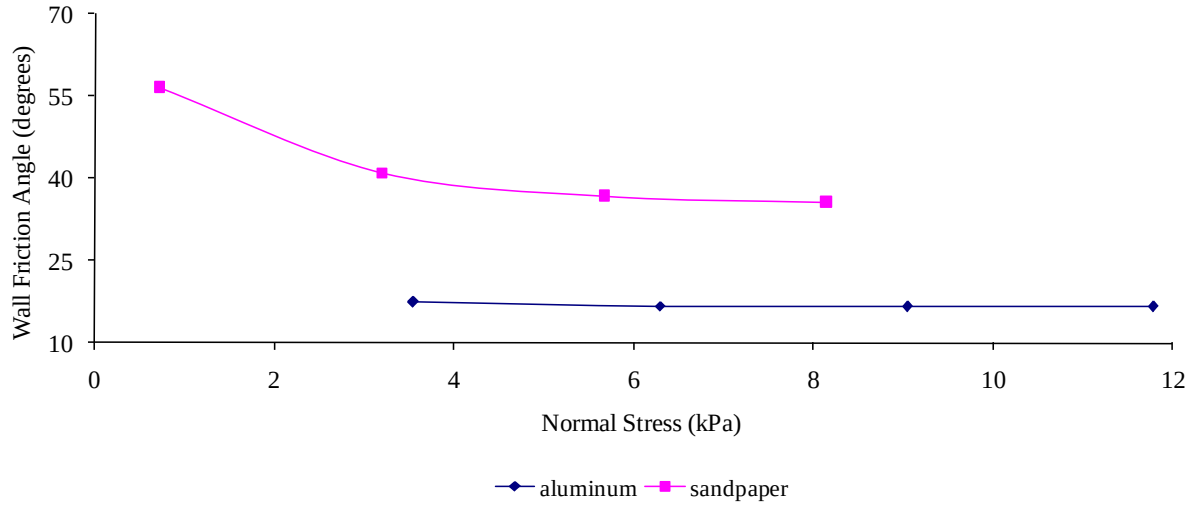

Figure 4-24. Wall friction angles for wheat flour on aluminum and sandpaper surface

Table 4-8. Flow properties measured by SJSC and ASC

Test method	Consolidation stress (kPa)	MPS (kPa)	UYS (kPa)	Angle of internal friction (degrees)	Effective angle of internal friction (degrees)
SJSC*	6.9	11.3	2.85	27.9	35.1
SJSC	6.9	10.5	2.24	29.0	34.9
ASC	7.5	11.9	6.46	31.3	48.3

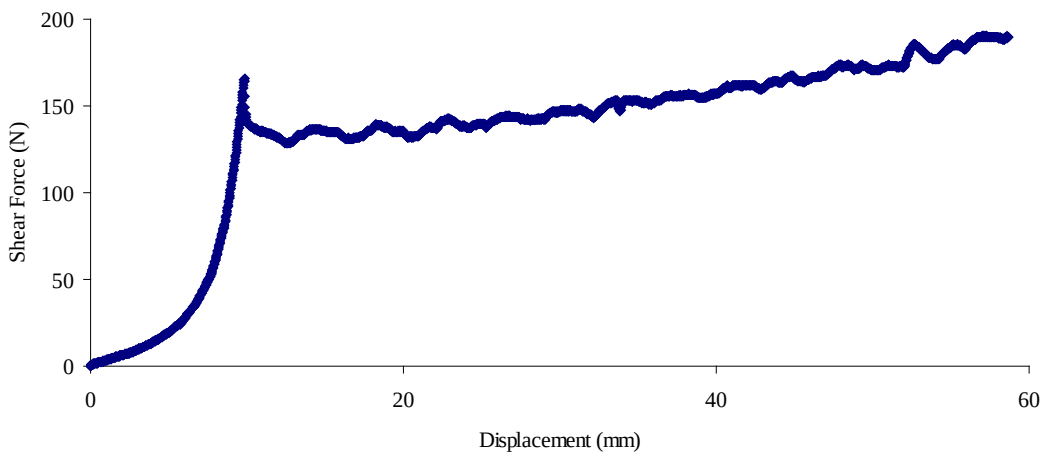

Figure 4-25. Force – displacement response of shear ring under 12 kPa of stress

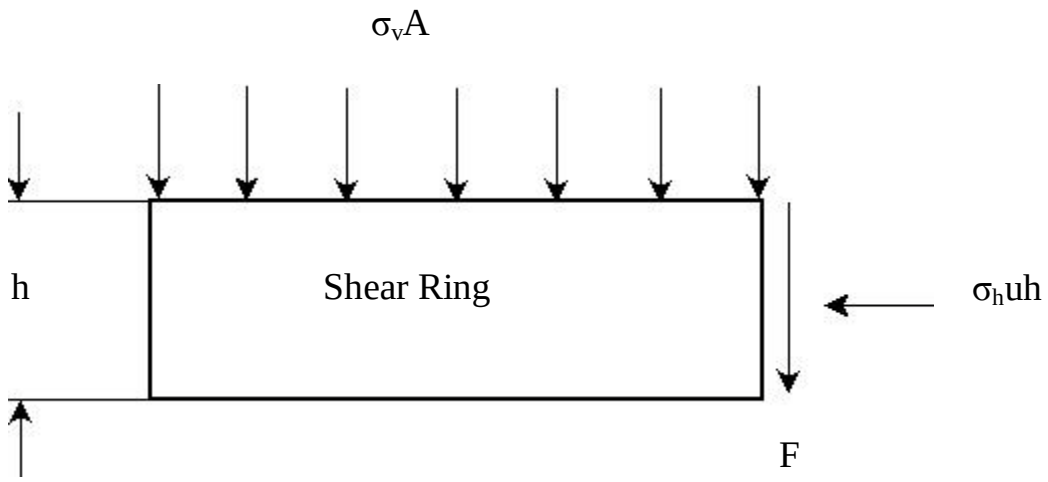

Figure 4-26. Force balance on the shear ring

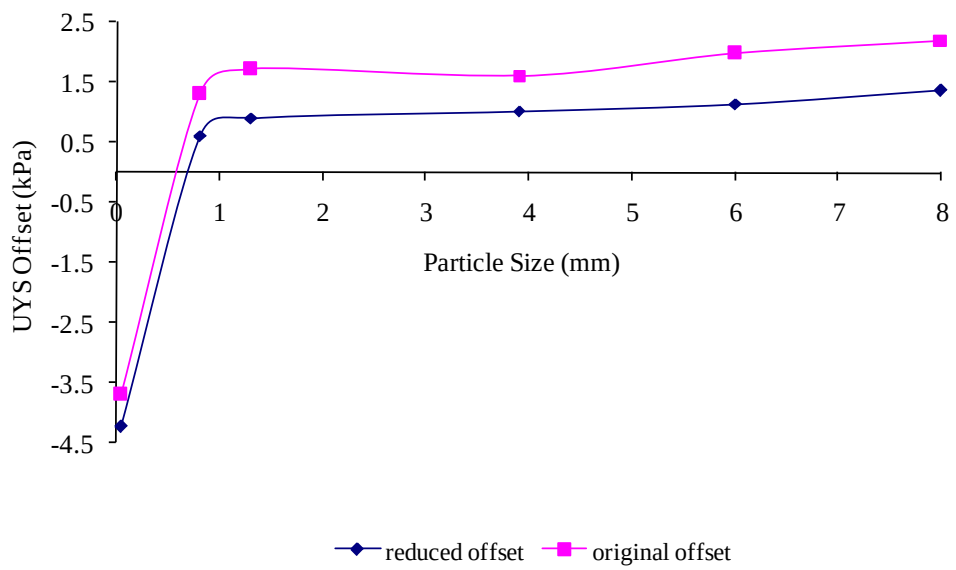

Figure 4-27. Effect of friction on the UYS offset

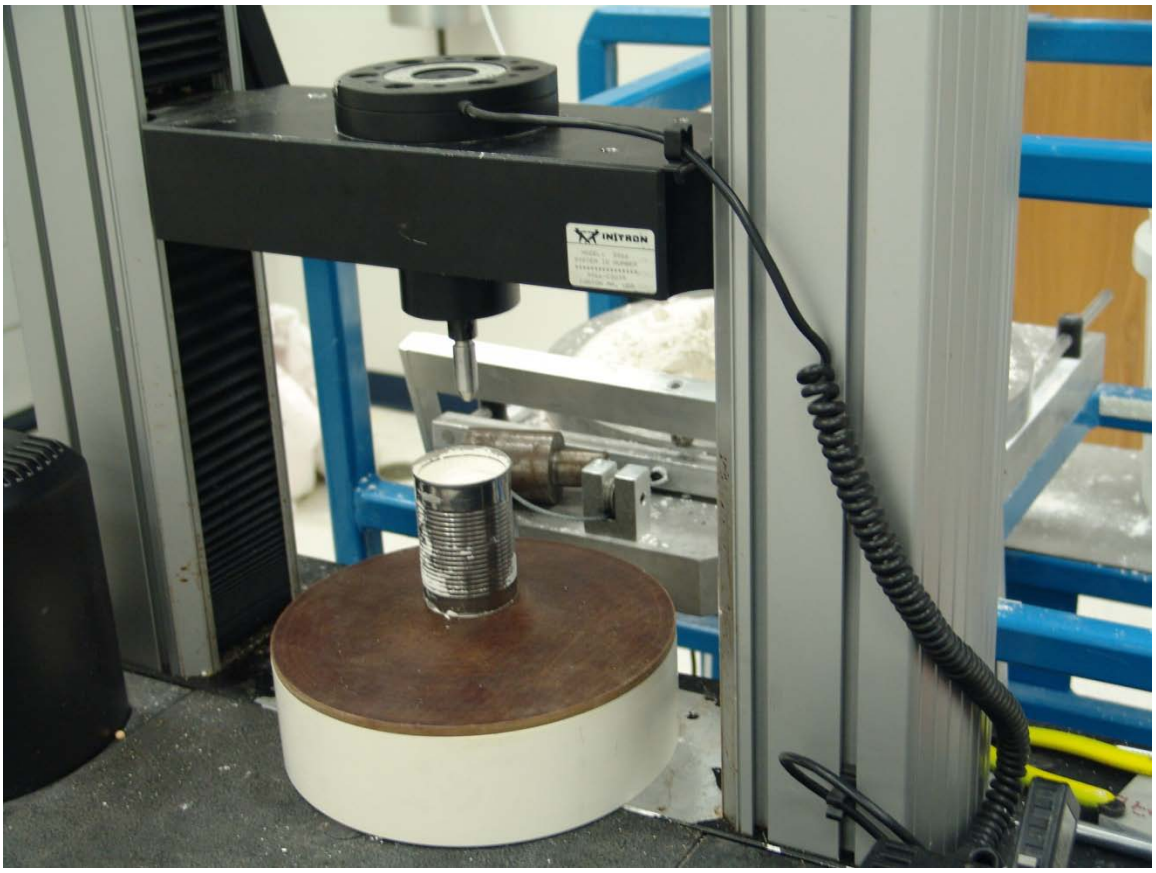

Figure 4-28. Penetration test set-up

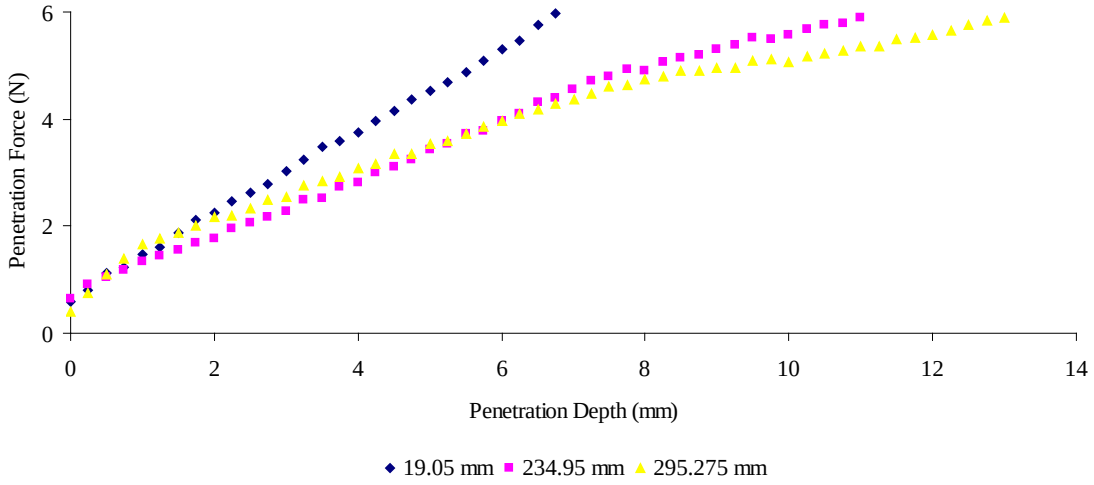

Figure 4-29. Typical penetration test data

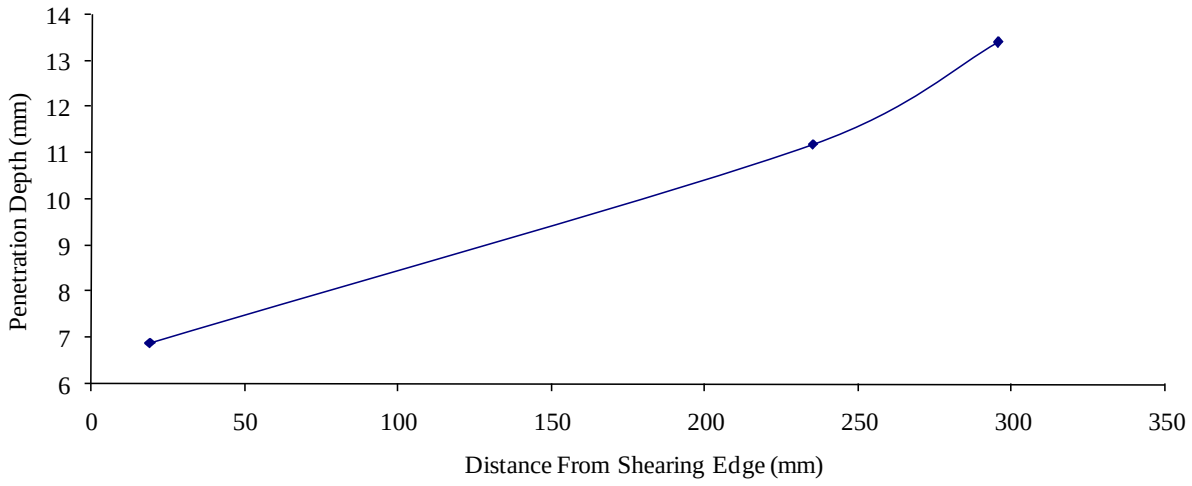

Figure 4-30. Variation in penetration depth with increasing distance from shearing edge

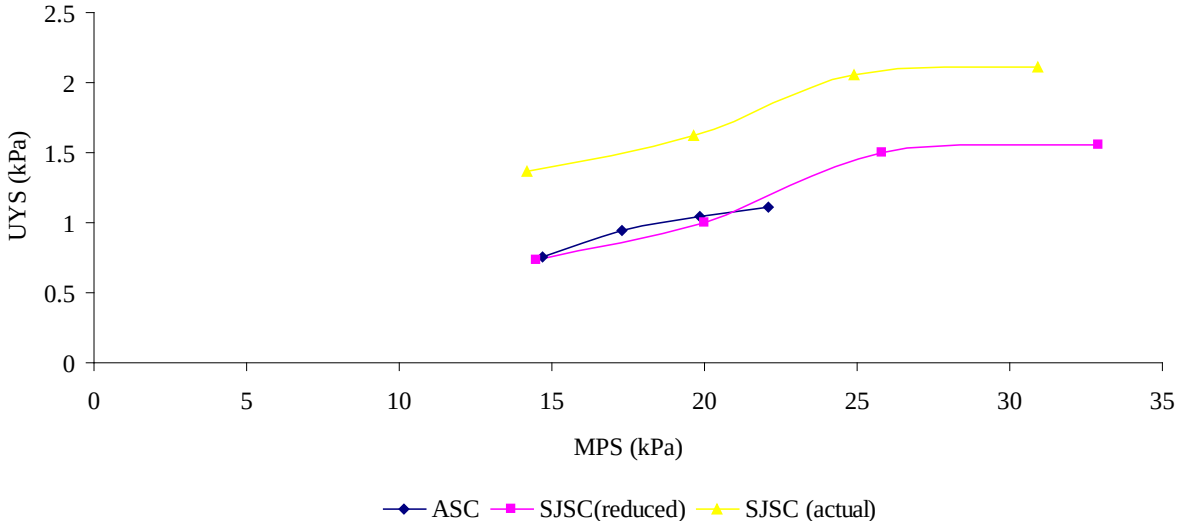

Figure 4-31. Flow functions obtained for cornmeal from the offset analysis

Table 4-9. Offset values of c and ϕ obtained from the offset analyses

Material	ϕ (degrees)	c (kPa)
Cornmeal	0.08	-137.5
Corn grits	1.3	-198.9
Mung beans	1.4	-288.9

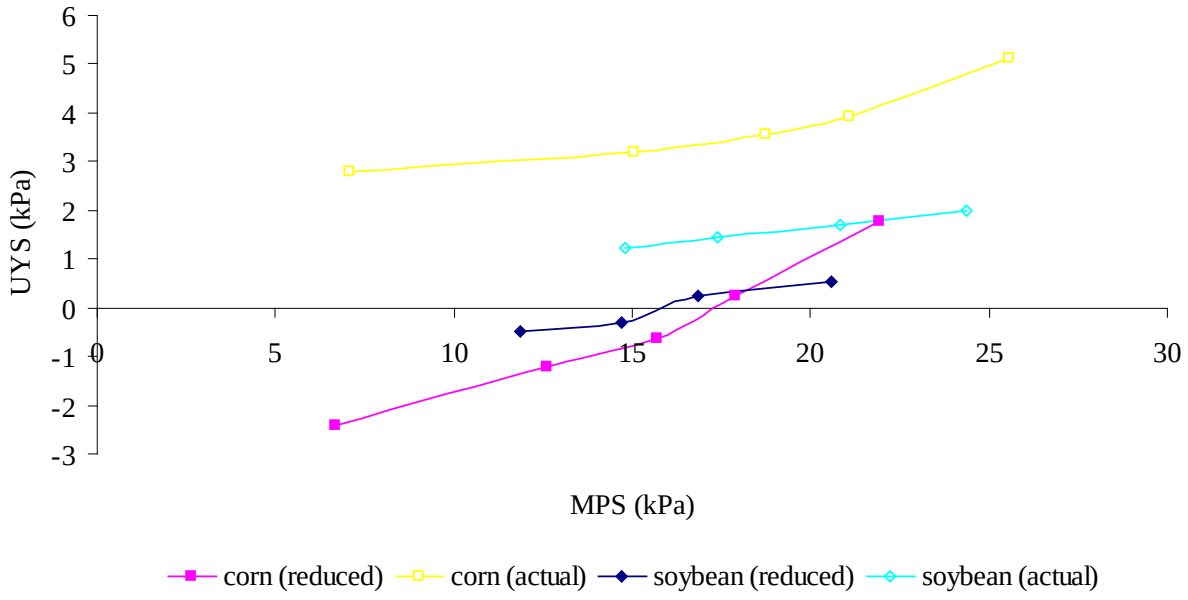

Figure 4-32. Flow function obtained for corn and soybean from offset analysis

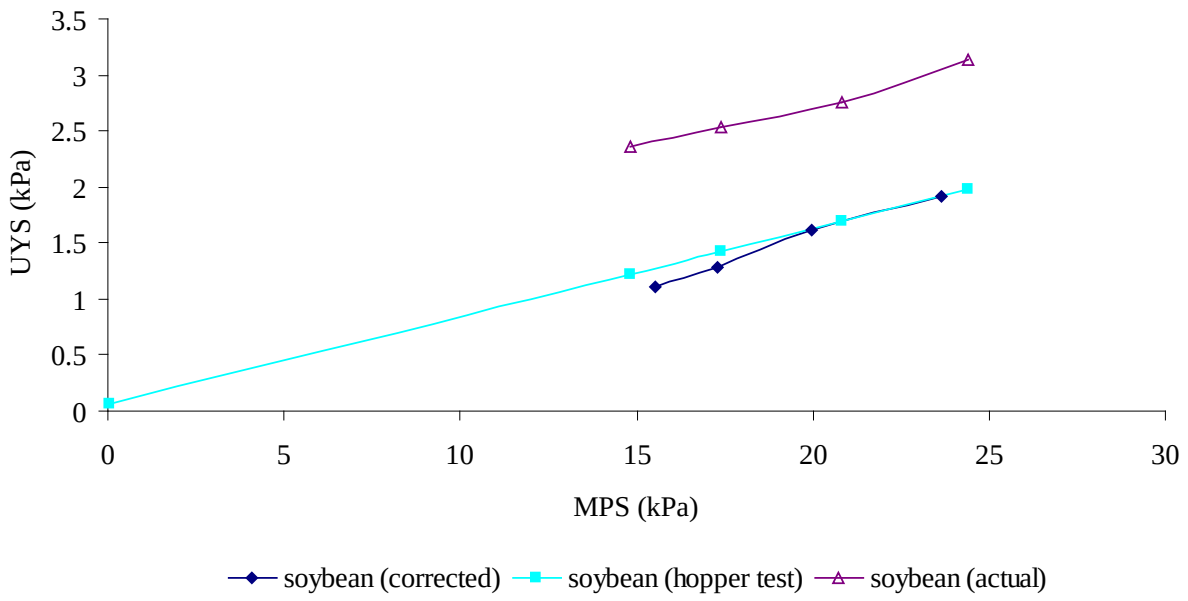

Figure 4-33. Flow function obtained for soybeans from offset analysis

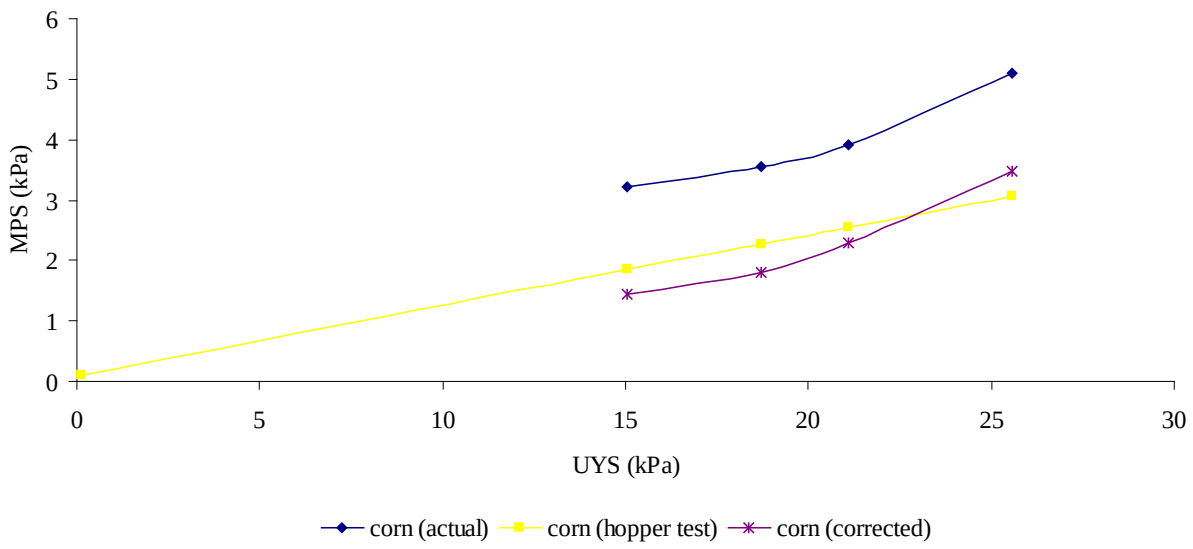

Figure 4-34. Flow function obtained for corn from offset analysis

CHAPTER 5
SUMMARY AND CONCLUSIONS

The first objective of the study was to determine whether the flow properties of bulk materials measured by the scaled up Jenike shear cell (SJSC) were equivalent to those measured by a standard Annular shear cell (ASC). Shear tests were performed on wheat flour, cornmeal, mung beans and corn grits to determine their flow properties using both the SJSC and the ASC. The test results showed that in comparison to the ASC, the SJSC gave lower unconfined yield strength values (UYS) for wheat flour but higher UYS values for cornmeal, mung beans and corn grits. A t-test revealed that the flow properties of the four test materials obtained from the SJSC were statistically different (at the 95% confidence interval) from the flow properties obtained through the ASC.

The second objective of this study was to evaluate the efficacy of the SJSC in determining the flow properties of large sized particles. Shear tests were performed on corn and soybeans using the SJSC; however, owing to their large particle size, they could not be tested on the annular shear cell. As a consequence, the flow functions of soybeans and corn obtained from the SJSC were compared with the flow functions obtained from experimental arching dimension tests on a conical hopper. The comparison revealed that the SJSC estimated significantly higher values of UYS for both corn and soybeans. These results were unanticipated. As a result based on the inconsistency between the flow property comparison between the ASC and the SJSC and flow function comparison between the SJSC and hopper tests for corn and soybeans it was concluded that the SJSC was ineffective in measuring flow properties of large particle sized bulk solids.

Possible factors causing the anomaly between SJSC and ASC data were also investigated Based on the factors investigated and analysis performed the following conclusions were drawn:

1. Friction in the SJSC geometry was a major concern. The contacts between the Teflon guides and steel rods and between the shear ring and base were identified as the major source of friction. The shear test data had to be adjusted to account for the frictional force.

2. For wheat flour, the low unconfined yield strength values (UYS) determined from the SJSC were attributed to normal stress variation that occurred when the wheat flour was sheared. The normal stress variation caused partial shearing and partial consolidation of wheat flour. Consequently, it was felt that it would be more practical to use the ASC for evaluating wheat flour properties. Also, more than three hours were required to obtain a single yield locus for wheat flour from the SJSC.

3. Results of the offset analysis for cornmeal and corn grits yielded relatively small offsets in cohesion (c) and angle of internal friction (ϕ) values. This indicated the sensitivity of the yield loci to relatively small changes in the measured shear forces. The offset in c can be attributed to a friction component between the bulk solid and the SJSC surface. If all the friction components in the tester can be rigorously accounted, the SJSC could give more accurate results.

4. Offset analysis facilitated normalizing the flow property data for corn and soybean with respect to the ASC, by applying cohesion (c) and angle of internal friction (ϕ) correction factors. Because, negative values of unconfined yield strength were obtained another data point was incorporated in the estimation of correction factors. But, due to the uncertainty in establishing an appropriate relationship between ϕ and particle size, it was felt that a better estimate of correction factors was required. To obtain accurate correction factors, more types of bulk solids should be tested on both the SJSC and ASC. Consequently, accurate correction factors could enable measuring flow property data of bulk solids incapable of being measured in the ASC due to large particle size.

This study provides an insight into the possible factors that should be considered while scaling a shear cell. However, at the end of the study, more questions were raised than were answered. Yet, the questions help define where the future efforts should be directed. Some of the avenues are highlighted below:

1. Vanes were introduced into the scaled-up Jenike shear cell (SJSC), to ensure a uniform distribution of shear and normal stresses in the shear cell. Since shear tests were performed on bulk solids with varying particle size, optimization of the number, and height of the vanes is required.

2. Cohesive bulk solids with large particle size should be tested on the SJSC. This would facilitate a comparison between flow properties of large particle sized - free flowing and cohesive bulk solids. Based upon the measured unconfined yield strength values a qualitative assessment of the SJSC's performance can be made.

3. It is assumed that the bulk solid behaves as a continuum in the shear cell. The major assumption in continuum mechanics is that the volume elements forming the continuum (the particles) should be very small compared to the volume of the continuum to be handled. As a result for measuring flow properties of coarser bulk solids, scaling-up of shear cells is justified. But scaling of the shear cell is based on an assumption that a certain number of particles would constitute a continuum. Alternatively, to assess the critical dimension of a shear cell for a specific bulk solid, more shear cells with dimensions between that of the standard Jenike shear cell and the SJSC could be fabricated, and comparative tests could be performed.

4. Other testers such as the annular shear cell, triaxial cell, or a simple direct shear cell (used in soil mechanics) could be scaled-up. It would be interesting to see what advantages or disadvantages these shear cells have over the SJSC.

The performance of the SJSC reflected on some of the problems associated with the standard shear cells that are largely unnoticed or un-questioned. Nevertheless, the SJSC served a qualitative purpose in understanding some of the issues associated with shear testing of bulk solids.

LIST OF REFERENCES

ASAE Standard (2003). Moisture Measurement Peanuts. *ASAE* S410.1. American Society of Agricultural Engineers, St. Joseph, Michigan

ASTM (1997). D6182. Standard shear testing method for bulk solids using the Jenike shear cell. In *Annual book of ASTM standards.* Philadelphia, PA, USA: American Society for Testing and Materials.

ASTM (2008)D6773. Standard shear test method for bulk solids using the schulze ring shear.tester. In *Annual book of ASTM standards.* Philadelphia, PA, USA: American Society for Testing and Materials.

Beckman C. (2005). Particle Size Analyzer, LS 230.

Bilgili E., Yepes J., Stephenson L., Johanson K., and Scarlett B. (2004). Stress inhomogeneity in powder specimens tested in the jenike shear cell: Myth or fact? *Particle and Particle Systems Characterization*, 21(4), 293-302.

Janssen H.A. (1895). Versuche uber getreidedruck in silozellen. *Zeitschrift des Vereines deutscher Ingenieure*, 39, 1045-1049.

Jenike A.W. (1961). Gravity flow of bulk solids. *Bulletin 108. Utah Engineering Experimental Station, University of Utah,* USA.

Jenike A.W. (1964). Storage and flow of solids. *Bulletin 123.Utah Engineering Experiment Station, University of Utah,* USA

Jenike A.W., Johanson J.R. (1969). On theory of bin loads. *Journal of Engineering for Industry, Transactions ASME,* 91(2), 339-344.

Jenike A.W., Johanson J.R., and Carson J.W. (1973). BIN LOADS - 3. MASS-FLOW BINS. *Journal of Engineering for Industry, Transactions ASME,*, 95 Ser B(1), 6-12.

Ketchum M.S. (Ed.) (1907). *The design of walls, bins and grain elevators.* McGraw-Hill, New York.

Kreyszig E. (2005). *Advanced Engineering Mathematics.* (9th edn.). Wiley, New York.

Mohsenin N.N. (1986). *Physical Properties of Plants and Animal Materials.* Gordon & Brown Science Publishers, New York.

Nedderman R.M. (1992). *Statistics and Kinematics of Granular Materials.* Cambridge University Press, Cambridge.

PTC. (2007). Mathcad, 14.

Roberts I. (1882). On the pressure of wheat stored in elongated cells or bins. *Engineering*, 34, 399.

Schulze D. (2008). *Powders and Bulk Solids: Behavior, Characterization, Storage and Flow.* Springer.

Schwedes J. (2003). Review on testers for measuring flow properties of bulk solids. *Granular Matter*, 5(1), 1-43.

Walker D.M. (1966). Approximate theory for pressures and arching in hoppers. *Chemical Engineering Science*, 21(11), 975-997.

Walters J.K. (1973). Theoretical analysis of stresses in axially-symmetric hoppers and bunkers. *Chemical Engineering Science*, 28(3), 779-789.

BIOGRAPHICAL SKETCH

Shrey Gupta was born in Kaithal India. At the age of five, his family moved to Chennai, a metropolitan city in Southern India. He completed his high school in 2002 and got admitted to the Department of Chemical Engineering at Vellore Institute of Technology. He graduated from VIT University in 2007.

He came to the U.S. in 2007 to pursue a MS degree in the Department of Material Science and Engineering. However, he obtained a research opportunity in the department of Agricultural and Biological Engineering under the supervision of Dr. Ray A. Bucklin and subsequently changed his department. He graduated with a masters degree in August 2009.